Measurement of rare isotopologues of nitrous oxide by high-resolution multi-collector mass spectrometry

Paul M. Magyar*, Victoria J. Orphan, and John M. Eiler

Division of Geological and Planetary Sciences, California Institute of Technology, Pasadena, CA 91125, USA

*corresponding author (magyar@caltech.edu)

Abstract

RATIONALE: Bulk and position-specific stable isotope characterization of nitrous oxide represents one of the most powerful tools for identifying its environmental sources and sinks. Constraining $^{14}N^{15}N^{18}O$ and $^{15}N^{14}N^{18}O$ will add two new dimensions to our ability to uniquely fingerprint N_2O sources. **METHODS:** We describe a technique to measure six singly and doubly substituted isotopic variants of N_2O, constraining the values of $\delta^{15}N$, $\delta^{18}O$, $\Delta^{17}O$, ^{15}N site preference, and the clumped isotopomers $^{14}N^{15}N^{18}O$ and $^{15}N^{14}N^{18}O$. The technique uses the Thermo MAT 253 Ultra, a high-resolution multi-collector gas source mass spectrometer. It requires 8-10 hours per sample and ~10 micromoles or more of pure N_2O. **RESULTS:** We demonstrate the precision and accuracy of these measurements by analyzing N_2O brought to equilibrium in its position specific and clumped isotopic composition by heating in the presence of a catalyst. Finally, an illustrative analysis of biogenic N_2O from a denitrifying bacterium suggests its clumped isotopic composition is controlled by kinetic isotope effects in N_2O production. **CONCLUSIONS:** We developed a method for measuring six isotopic variants of N_2O and tested it with analyses of biogenic N_2O. The added isotopic constraints provided by these measurements will enhance our ability to apportion N_2O sources.

Introduction

Nitrous oxide (N_2O) is a trace component of Earth's atmosphere (currently ~328 ppb), acts as a greenhouse gas,[1] and is the main source of reactive nitrogen species that contribute to depletion of stratospheric ozone.[2] Its concentration in tropospheric air is increasing at an average rate of 0.8 ppb/year, which motivates the study of its budget and its environmental biogeochemistry. N_2O is produced mainly by biological processes and consumed by both biological and stratospheric reactions.[3] The biological sources are believed to be primarily associated with the microbial processes of denitrification and nitrification, but the balance of these sources in the environment is poorly constrained.

In denitrification, the anaerobic respiration of nitrate and nitrite by bacteria, fungi, and archaea yields N_2O as an intermediate or final product.[4] Microorganisms capable of complete denitrification can further reduce N_2O to N_2. The aerobic oxidation of ammonia to nitrite by archaeal and bacterial nitrifiers also leads to to leakage of trace amounts of N_2O as a side product,[5-7] likely by different pathways in the bacteria and archaea.[8-11] Nitrifier-denitrification by ammonia oxidizing bacteria has also been shown to produce N_2O during the reduction of nitrite by the denitrification pathway.[12] In addition, abiotic chemical pathways have also been shown to produce N_2O under environmentally relevant conditions from a variety of nitrogen compounds, including some intermediates of nitrogen-cycling microbes.[13-16] Increases in atmospheric nitrous oxide are thought to be linked to the stimulation of some or all environmental N_2O sources, especially through the fertilization of agricultural fields.[17] Understanding the relative importance of each of these biological sources to environmental N_2O is a critical component for biogeochemical modeling and future mitigation of this greenhouse gas.

Stable isotope measurements can constrain the sources and sinks of N_2O. Because of the asymmetric structure of N_2O, there are three distinct sites for isotopic substitution: terminal N, central N, and O. The incorporation of the stable isotopes of nitrogen (^{14}N and ^{15}N) and oxygen (^{16}O, ^{17}O, and ^{18}O) into these three molecular sites yields twelve distinct isotopic variants of N_2O (see Table 1). All of the singly substituted isotopologues of N_2O have been measured in natural samples, yielding $\delta^{15}N$ (bulk $^{15}N/^{14}N$ ratio, averaged across both positions), $\delta^{18}O$, and $\Delta^{17}O$ values, and the position specific ^{15}N incorporation (site preference)[1]. Each of these parameters constrains different aspects of the natural budget of N_2O. For example, measurements of $\delta^{15}N$ combine information about metabolism and source of N;[18, 19] measurements of $\delta^{18}O$ values have been used to characterize substrate sources and exchange of N_2O precursors with water,[20-22] and measurements of $\Delta^{17}O$ values reflect the influence of mass-independent isotope effects in atmospheric reactions on O incorporated into N_2O.[23] These parameters have been used to characterize N_2O from microbial cultures, soils, waters, and in the atmosphere.[24]

Perhaps the most sophisticated stable isotope constraint on the biogeochemistry of N_2O arises from measurements of differences in $^{15}N/^{14}N$ ratio between the two distinct N sites.[25, 26] Position specific ^{15}N incorporation is typically reported as the site preference (SP; commonly expressed as $\delta^{15}N^{\alpha} - \delta^{15}N^{\beta}$, where α and β denote the central and outer nitrogen atoms, respectively). We will report the site preference as

$$SP = \left(\frac{^{15}R^{\alpha}_{SA}}{^{15}R^{\beta}_{SA}} - 1 \right) = \left(\frac{\delta^{15}N^{\alpha} + 1}{\delta^{15}N^{\beta} + 1} - 1 \right) \cong \delta^{15}N^{\alpha} - \delta^{15}N^{\beta} . \quad (1)$$

[1] $\delta = (R/R_{ref} - 1)$, where $R = ^{15}N/^{14}N$, $^{17}O/^{16}O$, or $^{18}O/^{16}O$, and R_{ref} refers to N_2 in air for $\delta^{15}N$ and VSMOW for $\delta^{17}O$ and $\delta^{18}O$.

66 This expression is close to equality at values of site preference near 0‰. The site preference in
67 natural and equilibrated samples can potentially vary by tens of per mil. When both site
68 preference and $\delta^{15}N$ values are far from 0‰, such variations can lead to deviations from equality
69 in equation 1 of several per mil. The isotopic composition of the α nitrogen is determined by
70 measuring the ratio of $^{15}N^{16}O$ to $^{14}N^{16}O$ in the NO^+ ions produced by fragmentation of N_2O in
71 the ion source of a mass spectrometer; $^{15}N/^{14}N$ of the β nitrogen is then calculated by mass
72 balance based on an independent measurement of the bulk $\delta^{15}N$ value of the full N_2O
73 molecule,[26] using the relationship

74 $$^{15}R = \frac{^{15}R^{\alpha} + {}^{15}R^{\beta}}{2}. \quad (2)$$

75 Site preference measurements have provided the most useful isotopic constraints on the
76 microbial sources of N_2O. In particular, measurements of pure cultures suggest that N_2O
77 produced by archaeal[6] and bacterial[27-29] nitrification can be distinguished from that produced
78 by bacterial denitrification.[28, 30] However, ^{15}N site preference (as well as other stable isotope
79 proxies measured to date) cannot distinguish between archaeal and bacterial nitrification, nor
80 between nitrification and fungal denitrification[31] nor between denitrification and nitrifier-
81 denitrification.[27, 29] Nevertheless, site preference has been deployed as a tool for estimating the
82 contributions of particular microbes to environmental samples.[30, 32-34] In addition, site
83 preference measurements of atmospheric N_2O have been used to describe the contributions of
84 stratospheric sinks and biological sources to regional and global budgets.[35, 36]

85 There are seven isotopic variants of N_2O that have not been measured previously, all of
86 which contain two or more rare isotopes. Such species are referred to as ‘clumped’ or ‘multiply-
87 substituted’ isotopologues.[37, 38] Measurements of the clumped isotope composition of CO_2,[39]

88 methane,[40] and oxygen[41] have been used for geothermometry[42, 43] and for studying kinetic
89 processes such as carbonate mineral growth forced by CO_2 degassing,[44] the formation and
90 cracking of ethane,[45] and the biologically-mediated generation of O_2[46] and methane.[40, 47] A
91 previous theoretical study has suggested that the multiply-substituted isotopologue $^{15}N_2{}^{16}O$ could
92 be used as a tracer of stratospheric processing.[48] In principle, such arguments could be raised
93 for all seven clumped isotopologues of N_2O because each has unique vibrational properties and
94 thus unique thermodynamic stability and chemical-kinetic rates. However, we are not aware of
95 any prior measurement of a clumped isotopologue of N_2O at natural abundances and useful
96 precision.

97 We describe here the development of mass spectrometric techniques to measure all singly
98 substituted N_2O isotopologues, plus the clumped isotopomers $^{14}N^{15}N^{18}O$ and $^{14}N^{15}N^{18}O$, on a
99 single sample of gas and in a single analytical procedure. This set of measurements is enabled by
100 high resolution gas source mass spectrometry using the Thermo MAT 253 Ultra.[49] We report
101 precision, accuracy, and standardization techniques for this method, and preliminary
102 measurements of biogenic N_2O from a cultured denitrifying bacteria. A forthcoming paper will
103 present measurements of the compositions of diverse natural, cultured and synthetic N_2O
104 samples.
105
106 **Systematics of clumped and position-specific isotope effects**
107 A common basis for standardization in clumped isotope geochemistry is a state in which
108 rare isotopes are randomly distributed among all possible isotopic variants of a molecule. (An
109 alternative approach for compounds that are not easily randomized or equilibrated in the

laboratory is to instead standardize relative to an arbitrary reference material; e.g., ethane[45]) For an isotopic variant of N_2O, *i*, deviations from a random distribution re reported as Δ_i values:

$$\Delta_i = \left(\frac{{}^{i}\mathrm{R}}{{}^{i}\mathrm{R}^{*}} - 1 \right) \quad (3)$$

where ${}^{i}\mathrm{R} = [i]/[{}^{14}\mathrm{N}_2{}^{16}\mathrm{O}]$ and ${}^{i}\mathrm{R}^{*}$ denotes the value of ${}^{i}\mathrm{R}$ predicted for that sample if rare isotopes are randomly distributed among all twelve possible isotopic variants. For the clumped isotopomers considered in this study, ${}^{14}\mathrm{N}{}^{15}\mathrm{N}{}^{18}\mathrm{O}$ and ${}^{15}\mathrm{N}{}^{14}\mathrm{N}{}^{18}\mathrm{O}$, the random distribution can be calculated from the ${}^{15}\mathrm{R}$ and ${}^{18}\mathrm{R}$ values of the sample:

$$\mathrm{R}^{*}_{{}^{14}\mathrm{N}{}^{15}\mathrm{N}{}^{18}\mathrm{O}} = \mathrm{R}^{*}_{{}^{15}\mathrm{N}{}^{14}\mathrm{N}{}^{18}\mathrm{O}} = {}^{15}\mathrm{R}\,{}^{18}\mathrm{R}. \quad (4)$$

Likewise, for position-specific ${}^{15}\mathrm{N}$ incorporation, a randomized distribution of ${}^{15}\mathrm{N}$ is defined to be a 'site preference' of 0‰, that is, $\delta^{15}\mathrm{N}^{\alpha} = \delta^{15}\mathrm{N}^{\beta}$.

At equilibrium, both clumping and position-specific isotope effects are described by homogeneous exchange reactions among isotopic variants of N_2O.[50, 51] As described by Wang et al.,[50] all position specific and clumped isotope effects for N_2O can be described by a set of eight such homogeneous isotope equilibria. Position specific ${}^{15}\mathrm{N}$ incorporation is described by the reaction:[50-52]

$${}^{15}\mathrm{N}{}^{14}\mathrm{N}{}^{16}\mathrm{O} \rightleftharpoons {}^{14}\mathrm{N}{}^{15}\mathrm{N}{}^{16}\mathrm{O}. \quad (5)$$

The equilibrium constant for this reaction is

$$K_{\alpha\text{-}\beta} = \frac{\left[{}^{14}\mathrm{N}{}^{15}\mathrm{N}{}^{16}\mathrm{O}\right]}{\left[{}^{15}\mathrm{N}{}^{14}\mathrm{N}{}^{16}\mathrm{O}\right]} = \frac{{}^{15}R^{\alpha}}{{}^{15}R^{\beta}}. \quad (6)$$

This equilibrium constant can be directly determined from measurements of the values of $\delta^{15}\mathrm{N}^{\alpha}$ and $\delta^{15}\mathrm{N}^{\beta}$, and can be related to the commonly reported measure of site preference as follows:

$$\ln K_{\alpha-\beta} \cong \left(K_{\alpha-\beta} - 1\right) \quad (7)$$

and, through the Taylor expansion of $\ln K_{\alpha-\beta}$:

$$\delta^{15}\mathrm{N}^{\alpha} - \delta^{15}\mathrm{N}^{\beta} \cong \left(K_{\alpha-\beta} - 1\right). \quad (8)$$

In this work, we will report site preference as calculated by equation 1, which means that for an equilibrated sample

$$\mathrm{SP} = \left(K_{\alpha-\beta} - 1\right). \quad (9)$$

The values for equilibrium constants such as equation 6 can be calculated through principles of statistical thermodynamics and are dependent only on temperature and the vibrational properties of the relevant isotopologues.[53, 54] Because the vibrational energy for $^{14}N^{15}N^{16}O$ is lower than that of $^{15}N^{14}N^{16}O$ at any given temperature, $^{14}N^{15}N^{16}O$ is favored at equilibrium and is enriched over $^{15}N^{14}N^{16}O$ by 45.7‰ at 300K.[51]

The species that contain one ^{15}N and one ^{18}O can be described by the following reactions:

$$^{14}N^{15}N^{16}O + {}^{14}N^{14}N^{18}O \rightleftharpoons {}^{14}N^{15}N^{18}O + {}^{14}N^{14}N^{16}O \quad (10)$$

$$^{15}N^{14}N^{16}O + {}^{14}N^{14}N^{18}O \rightleftharpoons {}^{15}N^{14}N^{18}O + {}^{14}N^{14}N^{16}O. \quad (11)$$

Each of these reactions corresponds to an equilibrium constant that depends on a concentration of a clumped isotopic species:

$$K_{^{14}N^{15}N^{18}O} = \frac{\left[^{14}N^{15}N^{18}O\right]\left[^{14}N^{14}N^{16}O\right]}{\left[^{14}N^{15}N^{16}O\right]\left[^{14}N^{14}N^{18}O\right]} \quad (12)$$

$$K_{^{15}N^{14}N^{18}O} = \frac{\left[^{15}N^{14}N^{18}O\right]\left[^{14}N^{14}N^{16}O\right]}{\left[^{15}N^{14}N^{16}O\right]\left[^{14}N^{14}N^{18}O\right]}. \quad (13)$$

The values of $\Delta(^{14}N^{15}N^{18}O)$ and $\Delta(^{15}N^{14}N^{18}O)$ can be determined from the three equilibrium constants in equations 6, 12, and 13 as described by Wang et al.[50] For all these reactions, the

150 random distribution, or a Δ_i value of 0‰, is approached at elevated temperatures and reached as
151 an infinite temperature limit.[50] The measurement of the sum of $^{14}N^{15}N^{18}O$ and $^{15}N^{14}N^{18}O$ at
152 mass 47 can be described by

153 $$\Delta_{^{14}N^{15}N^{18}O+^{15}N^{14}N^{18}O} = \left(\frac{R_{^{14}N^{15}N^{18}O+^{15}N^{14}N^{18}O}}{R^{*}_{^{14}N^{15}N^{18}O+^{15}N^{14}N^{18}O}} - 1\right). \qquad (14)$$

154 For the isotopomers $^{14}N^{15}N^{18}O$ and $^{15}N^{14}N^{18}O$ we define a parameter analogous to ^{15}N site
155 preference, which we call ^{18}O site preference ('SP_{18}'):

156 $$SP_{18} = \left(\frac{R_{^{14}N^{15}N^{18}O}}{R_{^{15}N^{14}N^{18}O}} - 1\right) = \left(\frac{\Delta\left(^{14}N^{15}N^{18}O\right)+1}{\Delta\left(^{15}N^{14}N^{18}O\right)+1} - 1\right). \qquad (15)$$

157 The ^{18}O site preference is equivalent to the equilibrium constant for the reaction

158 $$^{15}N^{14}N^{18}O \rightleftharpoons {}^{14}N^{15}N^{18}O. \qquad (16)$$

159 In most other isotopic systems where the measurement of clumped isotopologues have
160 been reported (CO_2, carbonate, O_2 and methane), equilibrium exchange reactions comparable to
161 those reviewed above form the basis for both calibrated geothermometers and an absolute
162 reference frame for reporting clumped species.[39, 40, 42, 55] It is likely that the major natural
163 processes that form N_2O do not permit attainment of homogeneous equilibrium with respect to
164 the proportions of isotopologues. Nevertheless, the predicted variation of equilibrium constants
165 with temperature represents a potential reference frame for both clumped and position specific
166 isotope effects, useful as means both of establishing an experimentally verifiable scale for
167 reporting isotopic variations (e.g., Dennis et al.[56]) and of recognizing and quantifying kinetic
168 isotope effects (e.g., Daeron et al.,[44] Stolper et al.,[45, 57] Wang et al.,[47] Yeung et al.,[46]). The
169 most common experimental procedure for equilibrating CO_2, the most commonly-studied
170 clumped isotope system, is heating at low pressures and a temperature of 1000°C. Under these

conditions N_2O decomposes rapidly. It is not clear that there is any lower temperature at which gaseous N_2O will exchange isotopes quickly enough to reach a homogeneous isotopic equilibrium but not decompose due to thermal instability. For this reason, we exposed N_2O vapor to high-surface area alumina (Al_2O_3) at 200˚C in an attempt to catalyze isotopic equilibration. Alumina has been shown to be a relatively poor catalyst for the decomposition of N_2O into N_2 and O_2, and it has been suggested that the mechanism for this decomposition proceeds through an adsorbed complex.[58, 59] We hypothesized that this mechanism might allow for the exchange of isotopes on reversible adsorption. The results section of this paper reports experiments confirming this hypothesis.

Another way to produce gases with predictable abundances of every isotopologue is through gas-phase diffusion at low pressures and temperatures, which we expect should follow relatively simple predictions of the kinetic theory of gases. Diffusive fractionations through low density gases can be described by either of two mass laws. When the mean free path of a molecule of diffusing gas is longer than the width of an aperture through which it diffuses, diffusion is described by the Knudsen diffusion law, where the fractionation factor for an isotopologue of mass m_i relative to some reference isotopologue with a different mass is a function of just the masses of the diffusing isotopologues:

$$\alpha_i = \frac{{}^{i}\mathrm{R}_{\mathrm{diffused}}}{{}^{i}\mathrm{R}_{\mathrm{residual}}} = \sqrt{\frac{m_{{}^{14}\mathrm{N}_2{}^{16}\mathrm{O}}}{m_i}}. \qquad (17)$$

Alternatively, at higher gas densities, where the mean free path is shorter, diffusion of N_2O isotopologues through N_2O (mostly composed of $^{14}N_2{}^{16}O$, assuming natural isotope abundances) is described by the mass law for gas-phase interdiffusion:[60, 61]

$$\alpha_i = \frac{{}^{i}\mathrm{R}_{\mathrm{diffused}}}{{}^{i}\mathrm{R}_{\mathrm{residual}}} = \sqrt{\frac{m_i + m_{^{14}\mathrm{N}_2{}^{16}\mathrm{O}}}{2m_i}}. \qquad (18)$$

For either Knudsen or gas-phase interdiffusion, the relationship between diffusive mass laws for two isotopologues, *i* and *j,* can be described by its 'mass law', or λ value, where

$$\alpha_{m_i} = \left(\alpha_{m_j}\right)^{\lambda_{m_j/m_i}}. \qquad (19)$$

Diffusive mass laws for N_2O predict modest but predictable increases in the clumped isotopic anomaly (Δ_i value) of diffused gas relative to residual gas.[37] Because isotopomers of N_2O, like $^{14}N^{15}N^{16}O$ and $^{15}N^{14}N^{16}O$, have identical masses, the kinetic theory of gases predicts that diffusive fractionations will not produce any site-preference isotope effects.

Both equilibration and diffusion produce predictable compositions of various isotopologues of nitrous oxide. Together they provide methods for producing predictable abundances of each isotopologue measured in this study, and thus a basis for evaluating the accuracy of our methods. In the results section, we will report the results for N_2O diffused through a small aperture and equilibrated at temperatures ≤200°C.

Sample Preparation

We purified samples of N_2O prior to mass spectrometric analysis by cryogenic distillation on a glass vacuum line. First, N_2O was frozen into a glass trap immersed in liquid nitrogen and exposed to a vacuum pump. This procedure removed non-condensable contaminants like O_2, N_2, and Ar. Second, the trap containing the sample was thawed to room temperature and water was removed by passage over a glass trap immersed in a slurry of dry ice and ethanol, which has a temperature of -60°C to -70°C. Third, biogenic samples and other gases with large amounts of CO_2 were purified by passage over ascarite (Ascarite-II, Thomas Scientific, Swedesboro, NJ,

214 USA); water generated by the reaction of CO_2 with ascarite was continually removed by a trap
215 immersed in a dry ice-ethanol slurry. Finally, samples that contain ethanol, methanol, and other
216 organic contaminants were cleaned by passage over a glass trap immersed in an ethanol
217 liquid/ice slurry, which was monitored to ensure that it has a temperature below -110°C.
218 To produce equilibrated N_2O, we heated samples in quartz breakseals at 200°C in the
219 presence of high surface area alumina (Sigma-Aldrich, St. Louis, MO, USA). About 200 mg of
220 alumina was placed in each breakseal and capped with quartz wool. The alumina was heated
221 with a natural gas torch under vacuum until the pressure in the system dropped to below 10
222 millitorr. Once the alumina cooled back to room temperature, about 80 micromoles of N_2O was
223 condensed into the tube by immersing its end in liquid nitrogen, and the tube was then flame
224 sealed with a torch. These tubes were then heated to 200°C for between 3 and 72 hours in a
225 Lindberg furnace, with temperatures monitored by a calibrated thermocouple. On removal from
226 the furnace, tubes were quenched by moving them through the air or placed in the flow of air
227 from an electric fan.[40] Once cooled to room temperature, the tubes were then attached to a
228 vacuum line using a tube-cracker device and broken to release N_2O. This N_2O was purified
229 cryogenically to remove any N_2 and O_2 that may have formed from N_2O; typical recovery of
230 N_2O was 90-100% of the amount condensed in the tube before heating. To generate N_2O
231 equilibrated at lower temperatures, we followed the preceding procedure, but with a first stage at
232 200°C for 12 hours followed by a second stage of 119 hours to 7 weeks duration, either in an
233 oven (93°C) or a constant-temperature water bath (either 25°C or 50°C). N_2O heated at a lesser
234 temperature without treatment at 200°C first does not exchange in timescales of hours to days; a
235 sample heated at 150°C for ~1 day exhibited unchanged values of all isotopic parameters and
236 100% of the initial N_2O was recovered. The initial heating step at 200°C appears to be necessary

for low-temperature catalysis. A possible explanation for this phenomenon is that the catalyst becomes activated, either by sustained heating at 200°C or by the presence of the small amounts of N_2 and O_2 evolved from the decomposition of N_2O (typically ~5% of the initial N_2O).

To fractionate gases by diffusion, we created a reservoir of N_2O gas (2 L; ≤10 torr) and let it leak to an evacuated vacuum line through a bellows-sealed needle valve (SS-4BMG; Swagelok, Solon, OH, USA) that was opened the least amount that permitted an appreciable flow of gas. Once gas passed through the valve it was immediately frozen into a glass trap immersed in liquid nitrogen. In each experiment, about 10% of the N_2O in the system was collected, over the course of about an hour, until ~20 micromoles of gas was obtained. Then, the needle valve was sealed and a similar amount of gas was sub-sampled from what remained in the reservoir and vacuum line, for determination of the isotopic composition of the residual N_2O. Both samples were cleaned cryogenically after collection, and were then flame sealed into Pyrex tubes for storage before analysis.

Biogenic N_2O was produced by cultures of the denitrifying bacterium *Pseudomonas aeruginosa* strain PA14, with a genetic knockout (Δ*nosZ*) of the gene for N_2O reduction, making N_2O the final product of denitrification. Triplicate cultures were grown in autoclaved 200 mL bottles containing 150 mL autoclaved, amended Luria-Bertani (LB) medium with 20 mM sodium nitrate (in one liter: 25 g LB mix, Difco, Sparks, MD, USA; 0.78 g KH_2PO_4; 2.50 g K_2HPO_4; and 1.72 g $NaNO_3$, Sigma-Aldrich). Each culture was inoculated with 1 mL aerobic liquid culture and grown until growth ceased, as determined by optical density measurements at 500 nm. At the end of growth, the gas in the headspace was expanded into an evacuated glass sampling volume connected to the bottle and separated from both the bottle and a vacuum line by

Teflon vacuum valves. The gas in this sampling volume was then expanded into a vacuum line, where noncondensible gases, CO_2, water, and hydrocarbons were removed as described above.

Measurement Techniques

The measurement technique described below builds on previously published methods for site-specific ^{15}N analysis of N_2O[26] and clumped isotope analysis of CO_2,[39] and makes use of a recently developed high resolution gas source isotope ratio mass spectrometer—the Thermo MAT 253 Ultra (Thermo Scientific, Bremen, Germany).[49] In particular, our method involves three separate analyses of singly and doubly substituted isotopologues of NO^+ fragment ions and N_2O^+ molecular ions, all done at mass resolutions of ~15,000-18,000 (using a 16 μm entrance slit), sufficient to mass resolve species of interest from contaminants (i.e., isotopologues of CO_2 or O_2 that are nearly isobaric with those of N_2O or NO, respectively) or nearly isobaric interferences among isotopologues of N_2O or NO (e.g., $^{15}N^{14}N^{16}O^+$ from $^{14}N_2{}^{17}O^+$).

The measurement of all isotopologues of interest of a single sample requires 8-10 hours, divided between instrument tuning, background measurements, analyses of isotopologues of NO, and analyses of isotopologues of N_2O. Figure 1 presents a summary of the steps required for the measurement. At the start of each day, the Ultra is tuned for sensitivity and resolution, using a 16 μm entrance slit and generally achieving a mass resolving power ($M/\Delta M$, 5/95 % definition) of 15,000-18,000. The most sensitive and important mass resolution problems we encounter are the separation of $^{15}N^{18}O$ from $^{17}O^{18}O$ at mass 33, which requires a mass resolution of ~6100; ($^{14}N^{15}N^{16}O$+$^{15}N^{14}N^{16}O$) from $^{14}N_2{}^{17}O$ at mass 45, which requires a mass resolution of ~6300; $^{14}N_2{}^{18}O$ from $^{15}N_2{}^{16}O$ at mass 46, which requires a mass resolution of ~4500; and ($^{14}N^{15}N^{18}O$+$^{15}N^{14}N^{18}O$) from $^{13}C^{18}O^{16}O$ at mass 47, which requires a mass resolution of ~9600.

For each set of measurements, detectors are positioned so that the flat tops of every peak of interest are aligned. This requires moving detectors between collection of NO^+ and N_2O^+ ions, as well as moving a single collector during the collection of N_2O to collect both ($^{14}N^{15}N^{16}O$+$^{15}N^{14}N^{16}O$) and $^{14}N_2{}^{17}O$ at mass 45. Unless otherwise noted, all measurements described below are collected in dual inlet mode (i.e., repeated comparison of a sample to a standard by cycling a changeover valve block), and every sample/standard comparison ('acquisition') is divided into 10 measurements of a sample, each of which is preceded and followed by a standard measurement. The integration time for each individual sample or standard measurement is 8 seconds.

For the first set of acquisitions, the magnet current and detector positions are set to simultaneously detect four isotopologues of NO, including $^{14}N^{16}O$, $^{15}N^{16}O$, $^{14}N^{18}O$, and $^{15}N^{18}O$. Masses 30, 31, and 32 are detected by Faraday cups (10^{10} Ω, 10^{12} Ω, and 10^{12} Ω amplifiers, respectively) and mass 33 by a secondary electron multiplier (see Figure 2). Under the assumption that all nitrogen in NO^+ fragment ions comes form the interior, α, site in N_2O, the measurements of $^{15}N^{16}O$ and $^{15}N^{18}O$ constrain the proportions of $^{14}N^{15}N^{16}O$ and $^{14}N^{15}N^{18}O$ respectively. This assumption will be tested and refined to account for fragmentation/recombination effects in a subsequent section. The measurement of $^{14}N^{18}O$ provides a constraint on the molecular $\delta^{18}O$ value. Eight acquisitions are collected in this configuration.

Second, the magnet current and detector positions are adjusted so that the detector array collects isotopologues of molecular N_2O^+, including $^{14}N_2{}^{16}O$, $^{14}N_2{}^{17}O$, $^{14}N_2{}^{18}O$, and the sum of $^{14}N^{15}N^{18}O$ and $^{15}N^{14}N^{18}O$. These measurements constrain the bulk molecular $\delta^{17}O$ value; provide a second, redundant constraint on the molecular $\delta^{18}O$ value; and constrain the total abundance of

both ^{15}N-^{18}O clumped species. Masses 44, 45, and 46 are detected by Faraday cups (10^{10} Ω, 10^{12} Ω, and 10^{11} Ω amplifiers, respectively) and mass 47 by a secondary electron multiplier, as shown in Figure 3. Six acquisitions are typically collected in this configuration.

Finally, the position of the mass 45 detector is slightly adjusted to measure the sum of $^{14}N^{15}N^{16}O$ and $^{15}N^{14}N^{16}O$, constraining the bulk molecular $\delta^{15}N$ value. The mass 45 ion beam is detected by a Faraday cup (10^{11} Ω or 10^{12} Ω amplifier). In this configuration, the measurement of $\delta^{18}O$ and the ^{15}N-^{18}O clumped species continues at masses 46 and 47. Two acquisitions are typically collected in this configuration, bringing the total number of acquisitions for $^{18}O/^{16}O$ and the ^{15}N-^{18}O clumped species to eight.

Before each acquisition, a 'mass scan' is collected by varying the magnetic field of the mass spectrometer to cover the region of the image plane where peaks of interest overlap and a magnet setting that is in the flat region for each peak is chosen for the measurement. Sample and reference bellows are pressure balanced manually to be at the same pressure as that scan. Immediately after each acquisition, a series of sixty-second background scans are collected for both sample and reference gases. Because ion beams are narrower than the detectors, it is possible to have two peaks that are formally resolved but are detected at the same time (see Figures 2-3). Therefore, CH_2F, methanol, ethanol, and/or other organic isobars can be collected with the NO or N_2O peaks, depending on exactly where peaks are positioned relative to collectors during analysis. To correct for the contributions of these contaminants that are formally resolved from but collected with the peak of interest, as well as for scattered ions and dark noise detected by electron multipliers, we collect scans just off the main peak, typically ~0.01-0.05 u from the measurement position, with the exact position chosen based on the mass scan collected before an acquisition. The signal associated with the interference is then

subtracted from the measured counts per second for each of the sample and reference measurements from the previous acquisition. The size of this correction is typically between 15% and 20% of the total signal measured at mass 33 and ~1% of the total signal measured at mass 47. At least once per cup configuration, scans are also collected to account for the non-zero baseline and dark noise observed on Faraday cups when gas is flowing but no ion beams are focused on a given detector. These scans are collected by choosing a magnet setting above and below the peaks for masses 30-32 and 44-46 (typically 0.1-0.15 u away from the measurement position) are averaged, and the results are subtracted from the observed voltage at the appropriate Faraday cup. These baseline corrections are typically between -2 and 2 mV, for voltages that range from ~100 mV ($^{14}N_2{}^{17}O$ measured using a 10^{12} Ω amplifier) to ≥10000 mV ($^{14}N_2{}^{16}O$ measured using a 10^{10} Ω amplifier).

There are two potentially significant interferences that are not mass resolved or accounted for by our background corrections: At mass 45, $^{13}C^{16}O_2$ is not resolved from ($^{14}N^{15}N^{16}O$+$^{15}N^{14}N^{16}O$). Therefore, it is necessary to monitor the relative amounts of CO_2 in the sample and reference gases, especially for biogenic gases, where N_2O and CO_2 are produced simultaneously. To estimate the amount of CO_2 in each sample, we measure the ratio of $^{12}C^{16}O_2$ to $^{14}N_2{}^{16}O$ at mass 44. The CO_2 signal is typically 0.6-0.8% of the N_2O signal for both sample and standard, and a given sample-standard pair is typically the same to within 2%. Offsets in pressure between sample and standard lead to an apparent variation in the contribution of CO_2 to the observed $\delta^{15}N$ value of 0.02‰ per percent change in the ratio $^{44}N_2O_{SA}/^{44}N_2O_{REF}$. As described above, CO_2 is removed from samples before they are introduced to the mass spectrometer by repeated passage over ascarite. Therefore, it is likely that CO_2 endogenous to the mass spectrometer is the main contributor to the observed N_2O/CO_2 ratios. The measurement of

standards described below constrain the accuracy and precision for $\delta^{15}N$ measurements, including any potential contribution from CO_2. Any sample with larger than-usual amounts of CO_2 can be re-scrubbed with ascarite and reanalyzed; CO_2 can typically be lowered to the level observed in standard gases. In addition, the hydride $^{14}N_2{}^{16}OH$, produced by reaction of N_2O with water in the ion source, is not fully resolved from $^{14}N_2{}^{17}O$. Therefore, it is necessary to dry samples cryogenically before introduction into the mass spectrometer, and to monitor the background levels of water.

Reproducibility and Standardization

Precision

The standard error of each individual measurement (the set of acquisitions described above) typically follows the expectation of counting statistics; Figure 4 shows the observed internal precision relative to the counting-statistics limit calculated for each of the measurements made on N_2O and the NO fragment. The number of counts varies with sample size, and precision varies correspondingly. For measurements of $\delta^{15}N$, $\delta^{17}O$, $\delta^{18}O$, and $\delta^{15}N^{\alpha}$, precision is typically better than 0.1‰. For measurements of $\Delta(^{14}N^{15}N^{18}O+{}^{15}N^{14}N^{18}O)$, typical values are between 0.1‰ to 0.4‰; and for SP_{18}, between 0.7‰ and 1.3‰. Replicate measurements of standard gases provide a measure of the external precision of the measurements. These values are reported in Tables 2 and 3 and are discussed further in in a subsequent section.

Calculation of 'scrambling factor' for $^{14}N^{15}N^{16}O$ and $^{15}N^{14}N^{16}O$

It has been established that reactions in the ion source scramble isotopes among isotopologues and isotopomers, leading to an interconversion of $^{14}N^{15}N^{16}O$ and $^{15}N^{14}N^{16}O$[25, 26,

[62, 63] We follow the approach of Toyoda and Yoshida[26] in correcting for this rearrangement by using a coefficient, y, to represent the fraction of ^{15}N atoms that switch positions in singly substituted isotopomers:

$$^{15}R^{\alpha}_{measured} = \left(1 - y\right)^{15}R^{\alpha}_{true} + y\,^{15}R^{\beta}_{true}. \quad (20)$$

This expression can be rearranged as

$$^{15}R^{\alpha}_{measured} = 2y\left(^{15}R - {}^{15}R^{\alpha}_{true}\right) + {}^{15}R^{\alpha}_{true} \quad (21)$$

where y varies from 0 for the case of no rearrangement among isotopomers, to 0.5 for the complete randomization of ^{15}N between $^{14}N^{15}N^{16}O$ and $^{15}N^{14}N^{16}O$, to 1 for the physically-unlikely scenario in which every $^{14}N^{15}N^{16}O$ becomes $^{15}N^{14}N^{16}O$ and vice-versa.

We constrained the value of 'y' for our instrument and method by analyzing two previously characterized interlaboratory standards: the Massachusetts Institute of Technology (MIT; Cambridge, MA, USA) reference gas, provided by Shuhei Ono, and our intralaboratory reference gas, for which the values of $\delta^{15}N$ and $\delta^{15}N^{\alpha}$ were measured at the Tokyo Institute of Technology (Yokohama, Japan) by Sakae Toyoda and Naohiro Yoshida. Comparison of our intralaboratory reference standard with the MIT reference gas, which has a preferred $\delta^{15}N$ of -0.24±0.01‰ and $\delta^{15}N^{\alpha}$ of -0.78±0.04‰, yields an apparent $\delta^{15}N^{\alpha}$ value for our reference gas of 6.80±0.16‰, 1 s.d. This measurement constrains the value of $^{15}R^{\alpha}_{measured}$. The independent analysis of our intralaboratory reference gas by the Tokyo Institute of Technology provides values of $\delta^{15}N^{\alpha}$ = 7.53‰ and $\delta^{15}N^{\beta}$ = 0.89‰ that imply corresponding values of $^{15}R^{\alpha}_{true}$ and $^{15}R^{\beta}_{true}$. Insertion of these three values into equation 20 allows us to solve for *y* on the Ultra at the tuning conditions used for this study as 11.0±0.2% (1 s.d.); all site preference results reported in this study use this value. Repeating this procedure by comparing our intralaboratory standard to

the Michigan State University (MSU; East Lansing, MI, USA) reference gas, provided by Nathaniel Ostrom, yields y = 10.8±0.3%. For comparison, previous observations of the scrambling factor range from 8.0% to 10.8%.[25, 26, 29, 64, 65]

Measurement of $\delta^{18}O$, $\delta^{15}N$ and $\delta^{15}N^{\alpha}$ values for interlaboratory standards

We tested the accuracy and full procedural reproducibility of our methods for isotopic properties that have been previously studied using other methods ($\delta^{18}O$, $\delta^{15}N$ and $\delta^{15}N^{\alpha}$) by repeated measurements of intra-laboratory and inter-laboratory N_2O standards. Our intra-laboratory standard, or 'working reference gas' was characterized for $\delta^{15}N$, $\delta^{15}N^{\alpha}$, and $\delta^{18}O$ values (4.21‰, 7.53‰, and 39.96‰, respectively) by S. Toyoda and N. Yoshida at the Tokyo Institute of Technology; their laboratory reference gas is itself standardized against inter-laboratory standards as described in Toyoda and Yoshida[26] and thus can be thought of as a secondary reference material. We also analyzed inter-laboratory standard gases provided by Stanford, MIT, and Michigan State University. The results of these measurements are reported in Table 2.

We find that $\delta^{15}N$ and $\delta^{18}O$ values for all standards match the reported values within the error of the two relevant measurements (i.e., ours and the independent constraint). In contrast, observed and reported $\delta^{15}N^{\alpha}$ values for interlaboratory standards that were not part of our calibration of the 'scrambling factor' (above) disagree with independently reported values by more than analytical precision (0.44 to 1.08 ‰ average discrepancy, vs. average external errors of 0.2 ‰). We do not have a conclusive explanation for these discrepancies, but in the subsequent section we describe one possibility that arises from our study of thermodynamically equilibrated samples. We also note that similar and greater disagreements in interlaboratory comparisons are a common feature of the current study of ^{15}N site preference in N_2O. A recent

community round-robin study determined the site preference of a single N_2O standard in eleven labs and found it to range from 16.6‰ to 25.4‰ (recalculated according to equation 1), even when the measurement of this gas was standardized to accepted reference gases and all data were subjected to a common correction procedure.[66] This inconsistency among laboratories is arguably the greatest challenge to current studies of the stable isotope geochemistry of N_2O, and motivated us to include in this work two experiments that offer some prospect for independent experimental verification of the accuracy of measurements of site preference and clumped isotope properties of N_2O, preferably through some procedure that could be repeated in all laboratories working in this field (i.e., by analogy with the use of heating and water-equilibration experiments to calibrate clumped isotope measurements of CO_2 by Dennis and coworkers[56]). The following sections describe two such experiments: equilibration over a heated catalyst, and diffusive fractionation.

Thermodynamically equilibrated samples and an absolute reference frame

One of the challenges of establishing new methods for measuring intramolecular isotopic distributions, such as site preference and clumping, is determining an absolute reference frame for reporting isotopic variations. In the cases of CO_2 (including CO_2 from carbonate), O_2 and methane, this has been done by driving these compounds to an equilibrated state at known temperature, and assuming that state corresponds to the isotopic distribution predicted by statistical thermodynamic theory. We have attempted the same approach with N_2O by heating gases over alumina, in the hope that this will drive them to equilibrium in their position specific and clumped isotope compositions with minimal disproportionation.

These experiments provide three tests of the attainment of equilibrium. First, as shown in Figures 5-7, we established that gases that differ from one another in initial SP, SP_{18}, and $\Delta(^{14}N^{15}N^{18}O+^{15}N^{14}N^{18}O)$ converge to common values of each of these parameters after heating in the presence of alumina catalyst, and then maintain that value irrespective of the amount of time at that temperature. The experiments performed at 200°C demonstrate both bracketing and time-independence—key benchmarks for proving a thermodynamically equilibrated state has been reached. Second, while we have not shown that the experiments performed at lower temperatures meet these criteria for equilibrium, Table 4 shows that they achieve even larger values of the site preference index, consistent in direction and order of magnitude with theoretical predictions. Notably, the difference between the sample heated to 93°C and the bracketed value at 200°C, after correction for the 'scrambling' effect described above, is 10.7±0.4‰, indistinguishable from the predicted difference at equilibrium of 10.65‰.[50, 51] The samples exposed to alumina at 25°C and 50°C approach but do not reach the predicted composition; we infer this to simply reflect the failure of these lower temperature experiments to fully reach equilibrium due to the greater kinetic inhibitions to exchange reactions (though perhaps longer time-series studies could document eventual equilibration at these lower temperatures). Finally, a less direct but still relevant observation is that the measurement of triple oxygen isotope compositions of heated samples are consistent with an equilibrium that involves exchange of oxygen between the N_2O and some component of the experimental apparatus. As is shown in Figure 7, N_2O samples with unusual oxygen isotope compositions ($\Delta^{17}O > 0$) evolve on heating toward a $\Delta^{17}O$ of 0‰ (although they do not quite reach 0‰). This suggests N_2O is exchanging oxygen with alumina, adsorbed water and/or glass during heating. If, instead, the changes in isotopic composition these samples undergo during heating were caused by some kinetic isotope effect (say, associated with minor amounts of

464 N_2O disproportionation), they would instead evolve along a line in $\delta^{17}O$-$\delta^{18}O$ space controlled by
465 the mass law of that fractionation (likely with a slope of ~0.515). In that case, $\Delta^{17}O$ would remain
466 approximately constant. The fact that an equilibrium is reached in intramolecular isotopic
467 distribution without achieving a $\Delta^{17}O$ of exactly 0‰ suggests that the reservoir of exchangeable
468 oxygen in the experimental apparatus is large, but not large enough to completely buffer the
469 oxygen in the N_2O.

470 If we are correct that heating N_2O when exposed to alumina drives it to thermodynamic
471 equilibrium with respect to the SP index on laboratory timescales, this procedure may provide a
472 basis for resolving (or at least exploring) interlaboratory discrepancies in SP measurements. That
473 is, each lab should be capable of generating N_2O equilibrated at two or more known temperatures
474 (and thus known values of the SP index); measurement of these standards should permit the
475 construction of lab-specific transfer functions relating measured to absolute values of that index
476 (much as for the absolute reference frame for clumped isotope analyses of CO_2).[56] Based on the
477 results of this study, the principal limitation of this approach would be the relatively poor
478 experimental reproducibility of our exchange experiments (e.g., corrected values of SP for long-
479 duration, 200°C experiments have a standard deviation of ±0.4‰). Nevertheless, it seems possible
480 to us that a concerted effort to refine this experiment could improve its reproducibility to levels
481 similar to the nominal state of the art for SP measurements (as good as ±0.05‰, omitting the
482 several-per-mil systematic errors that seem to affect interlaboratory comparisons).
483
484 *Standardizing $\Delta(^{14}N^{15}N^{18}O+^{15}N^{14}N^{18}O)$ and SP_{18} with equilibrated N_2O*

485 Having demonstrated that heating in the presence of a catalyst drives N_2O to internal
486 equilibrium with respect to the independently calibrated, conventional site preference, we use the

same experiments to establish an absolute reference frame for the new measurements of $\Delta(^{14}N^{15}N^{18}O+^{15}N^{14}N^{18}O)$ and SP_{18}. In particular, we assume that N_2O heated in the presence of alumina catalyst until it reaches a time-invariant composition has achieved equilibrium with respect to all of the isotope exchange homogeneous equilibria presented in Wang et al.[50]

A measurement of either of our new measured properties may be compromised by the same 'scrambling' effect described above for conventional site preference. This effect is expected to be small for $\Delta(^{14}N^{15}N^{18}O+^{15}N^{14}N^{18}O)$, where interconversion between $^{14}N^{15}N^{18}O$ and $^{15}N^{14}N^{18}O$ will not be detected because it involves no change in the total abundance of species with this mass. Only ion source scrambling reactions that change the relative abundance of the other 10 isotopologues will effect the observed $\Delta(^{14}N^{15}N^{18}O+^{15}N^{14}N^{18}O)$. We have no evidence indicating this occurs to measureable extents: the $\Delta(^{14}N^{15}N^{18}O+^{15}N^{14}N^{18}O)$ values of our equilibrated samples are within error of one another and broadly within the limited range of equilibrium values (Figure 8). Therefore, while we develop a correction for the effect of ion source 'scrambling' on SP_{18}, we provisionally assume measurements of $\Delta(^{14}N^{15}N^{18}O+^{15}N^{14}N^{18}O)$ are accurate once standardized against a gas equilibrated to 200°C, using the predicted thermodynamic result from Wang et al.[50] (see Table 4). It seems unlikely to us that this assumption could be in error by more than the analytical precision in this variable, but this issue should be re-visited in future work as we discover materials that vary more widely in this index.

It seems likely to us that the scrambling factor for SP_{18} is indistinguishable from that for SP, simply because it is difficult to think of a reason why the ^{18}O–^{16}O substitution would substantially change the rate of this interconversion. In principle, it should be possible to correct the scrambling effect for both SP and SP_{18} using equilibrated samples because if we have N_2O

that has been equilibrated at two or more temperatures, we can solve for the values of a scrambling correction coefficient that results in the theoretically predicted difference in composition between those temperatures.[50, 51] We cannot perform such a calibration with any confidence here because we have only demonstrated bracketing and time-invariance at one temperature (200°C). However, we illustrate the principles behind such a calibration, and examine whether our experimental data at lower temperatures are broadly consistent with the assumption that scrambling occurs at the same rate for SP and SP_{18}.

A linear array of samples with expected and measured compositions (see Figure 9) is described by

$$\Delta_i^{\text{measured}} = f \cdot \Delta_i^{\text{expected}} - \Delta_i^{\text{reference}}, \qquad (22)$$

where the factor f describes the sample process of scrambling as the factor y described above, and $\Delta_i^{\text{reference}}$ is the difference between the Δ_i of the reference gas and the Δ_i of a random distribution. The slope, f, in this space is related to scale compression ($f > 1$) or expansion ($f < 1$) due to rearrangement of atoms among isotopomers; a slope of 1 corresponds to no rearrangement, a slope of 0 to randomization of ^{15}N between α and β positions. To correct isotopomeric composition for scrambling, we use the expression

$$\Delta_i^{\text{corrected}} = \frac{\Delta_i^{\text{measured}}}{f} + \Delta_i^{\text{reference}} \qquad (23)$$

.

This correction procedure is presumed to account for the same ion source rearrangement process as the correction of Toyoda and Yoshida,[26] although we have adopted a mathematical formalism based on the Dennis et al.[56] absolute reference frame for CO_2 clumped isotope analysis. To demonstrate the relationship between these alternative approaches, we use our equilibrated samples to describe the rearrangement of $^{14}N^{15}N^{16}O$ and $^{15}N^{14}N^{16}O$. First, to

describe these samples, we introduce a parameter Δ_α, which is related to $\delta^{15}N^\alpha$ and is analogous to a clumped-isotope Δ value as defined in equation 3:

$$\Delta_\alpha = \left(\frac{^{15}R^\alpha}{^{15}R} - 1 \right). \qquad (24)$$

The bulk isotopic composition of a sample, ^{15}R, is also the composition that will be observed for both the α and β in the case of a random distribution of ^{15}N among the sites.

Taking equations 22 and 24 together, we find that

$$f = \frac{^{15}R^\alpha_{\text{measured}} - {}^{15}R}{^{15}R^\alpha_{\text{expected}} - {}^{15}R}, \qquad (25)$$

and by substituting equation 21 for $^{15}R^\alpha_{\text{measured}}$ in equation 25 ($^{15}R^\alpha_{\text{expected}}$ in equation 25 is equivalent to $^{15}R^\alpha_{\text{true}}$ in equation 25) we can solve for f in terms of y:

$$f = 1 - 2y. \qquad (26)$$

This factor varies from 1 when there is no rearrangement of isotopes among isotopologues (y=0) to 0 when there is a complete scrambling between $^{14}N^{15}N^{16}O$ and $^{15}N^{14}N^{16}O$.

Equilibrated samples at 200°C and 93°C offer an independent test of our estimation of the scrambling factor y. As shown in Figure 9, we find that f = 0.770±0.011, which corresponds to y = 11.5±0.6%, consistent with the value estimated from measurements of interlaboratory reference gases, as explained above. It is also shown in Figure 9 that when the equilibrated samples are corrected using the procedure described above, which is independent of the equilibration experiments, they approach a slope of 1, corresponding to no rearrangement.

Another point of comparison for this result comes from measurements of Δ_{47} in carbon dioxide, where the slope of the empirical transfer function described in Dennis et al.[56] is analogous to the inverse of the compression factor f. The range of slopes reported for various

laboratories performing Δ_{47} measurements is 0.87 to 0.99; all of these values are consistent with less scrambling of mass 47 carbon dioxide isotopologues than of nitrous oxide isotopomers. We also observe a y-intercept of -0.53±0.15, which can be interpreted as an offset between the expected and observed $\delta^{15}N^{\alpha}$ composition of the reference gas of 0.53±0.15‰.

When we follow an analogous procedure for SP_{18}, we observe a value of $f_{14N15N18O}$ of 0.48±0.10, which suggests a much larger likelihood for rearranging ^{18}O-containing isotopomers than ^{16}O-containing isotopomers. We consider this improbable, given the generally small effect of oxygen isotope substitutions on rate constants for common chemical reactions (on the order of one per cent). In addition, when this correction is applied to samples heated at 25°C and 50°C, a SP_{18} in excess of the thermodynamically-predicted value is produced even though SP measurements suggest that these samples have not reached equilibrium (Table 4). Therefore, we conclude that while the sample heated at 93°C may have reached (or at least closely approached) equilibrium in SP, it has not reached equilibrium in SP_{18}. This is plausible because we only performed detailed bracketing and time-series experiments at 200°C, so only at that temperature can we confidently make the interpretation that gases reached an equilibrium distribution in their isotopic composition. If there is a difference in kinetics between the SP and SP_{18} indices, it might be the result of slower rates for N-O bond reordering than for N-N bond reordering. In any event, we believe the temperature dependence of our exchange experiments does not produce a self-consistent and reasonable calibration of site-preference scrambling.

Instead, we assume that rate of rearrangement is the same for both SP and SP_{18}. In other words, we use $f = 0.77\pm0.011$ in equation 23 to adjust measured $\Delta(^{14}N^{15}N^{18}O)$ values. For the replicated and bracketed results at 200°C we then take the $\Delta(^{14}N^{15}N^{18}O)$ composition of the reference gas as the difference between that calculated quantity and the predicted value for

200°C. Then, using this result and the value for $\Delta(^{14}N^{15}N^{18}O+^{15}N^{14}N^{18}O)$ of the reference gas determined above, we solve for $\Delta(^{15}N^{14}N^{18}O)$ of the working gas (Table 5). As shown in Figure 10, samples heated to temperatures of 25°C and 50°C approach equilibrium compositions in SP_{18}, but they do not obtain equilibrium; this result matches our expectation from SP measurements. Notably, we see that the most anomalous result is the SP_{18} value for the 93˚C equilibration experiment—reinforcing our suspicion that this measurement produced an implausible result.

Diffusion experiments

A second way we can validate our new measurements is to generate fractionations of known amplitudes and/or mass laws through experimental manipulations of analytes; and then to see whether measured changes in composition, after correction for known artifacts such as ion source scrambling, match independent constraints or theoretical predictions. We performed three experiments in which N_2O was diffused through a needle valve and diffused and residual gas were collected and measured. We do not know the size of the aperture through which the gas was diffused. Therefore we cannot be sure whether experiments were conducted in the Knudsen diffusion or gas-phase interdiffusion regime (and in each experiment it could be different). In every case, the measured fractionations between diffused and residual gas are between the predictions for these two end-member possibilities, suggesting that the experimental setup is in an intermediate regime with respect to the ratio of aperture diameter to gas mean free path (i.e., a Knudsen number near one). For this reason we do not have a prediction of the amplitude of the experimentally generated diffusive fractionation. However, since the mass laws for Knudsen and gas-phase interdiffusion are closely similar, we can predict the mass law of the fractionation.

599 Then, we can use the observed difference between diffused and residual gases in values of $\delta^{18}O$
600 (a measurement we have already established is measured accurately and precisely by our
601 techniques) to calculate expected differences between diffused and residual gases for the values
602 of $\delta^{15}N$, $\delta^{17}O$, site preference, $\Delta(^{14}N^{15}N^{18}O+^{15}N^{14}N^{18}O)$ and clumped isotope site preference. We
603 compare these predictions to our measured results in Figure 11. Experiments 1 and 2 date from
604 before the introduction of complete background corrections for $\delta(^{14}N^{15}N^{18}O)$ and
605 $\delta(^{14}N^{15}N^{18}O+^{15}N^{14}N^{18}O)$ and therefore results are shown only for $\delta^{15}N$, $\delta^{18}O$, and $\delta^{15}N^{\alpha}$
606 measurements. Experiment 3 includes the appropriate background correction for CH_2F, CH_3OH,
607 and other isobars on $^{15}N^{18}O$ at mass 33, and is the only one of the three made with sufficient
608 control on the partial pressure of water in the ion source, which is important for achieving the
609 best accuracy and precision for measurements of $\delta^{17}O$. We find the scrambling-corrected
610 differences in composition between residual and diffused gas agree with the mass law of the
611 kinetic theory of gases, within the nominal errors of each measured isotope ratio. However, it is
612 important to note that since the final result is the difference between a diffused and residual
613 gases, it is not sensitive to small variations in the scrambling coefficient. These results
614 demonstrate the ability to measure all isotopologues, including those for which no standards
615 exist, with accuracy.
616
617 **Representative measurements of biogenic N_2O**
618 In Table 6 we report the $\delta^{15}N$, $\delta^{18}O$, $\Delta^{17}O$, SP, SP_{18}, and $\Delta(^{14}N^{15}N^{18}O+^{15}N^{14}N^{18}O)$ values
619 for nitrous oxide produced by the denitrifying bacterium *Pseudomonas aeruginosa* strain PA14
620 Δ*nosZ*. Because these bacteria lack the enzyme for nitrous oxide reduction, the isotopic
621 composition of nitrous oxide that accumulates in their cultures does not reflect any N_2O

consumption reactions.[67] The measurements of $\Delta(^{14}N^{15}N^{18}O+^{15}N^{14}N^{18}O)$ and SP_{18} values from these samples provide the first determination of the clumped isotope fingerprint of a biogenic N_2O source.

The conventional site preference (SP) measurements for these samples, –3.67±0.25‰, match previous measurements of N_2O from bacterial denitrifiers (–0.5 to –5.7‰[28, 30]). While the values of $\Delta(^{14}N^{15}N^{18}O+^{15}N^{14}N^{18}O)$ for these gases are consistent with thermodynamic equilibrium near room temperature (0.4‰ at 20°C), the observed values of SP and SP_{18} are not consistent with homogeneous equilibrium at any temperature.[50] Therefore the full, 6-dimensional stable isotope 'fingerprint' demonstrates that at least one step in that synthesis is an irreversible reaction that expresses a kinetic isotope effect. Using prior understanding of the mechanisms of N_2O biosynthesis in denitrification, we may be able to reach more specific conclusions: values of SP and SP_{18} must be set at the point when the N_2O molecule is synthesized by a nitric oxide reductase enzyme. As these properties violate equilibrium, we should conclude that this particular forward reaction expresses a kinetic isotope effect. Our results present a target for fitting mechanistic models of this reaction step.

On the other hand, $\Delta(^{14}N^{15}N^{18}O+^{15}N^{14}N^{18}O)$, a property that approaches or equals equilibrium in these samples, is influenced by the abundance of ^{15}N-^{18}O bonds, and may record information set at any of several steps in N_2O synthesis where N-O bonds are formed or exchanged: from the nitrate provided as a substrate, or from any (or all) of the three reductive reactions from nitrate to nitrite to nitric oxide to nitrous oxide. If any of these reactions is highly reversible or involves equilibration with water, as is commonly observed in denitrification,[68] there is the possibility that the distribution of ^{15}N-^{18}O bonds achieves an equilibrium composition in that step and that this equilibrium is not disturbed by the kinetic isotope effects controlling the

final step of formation of N—N bonds, and is therefore recorded in the $\Delta(^{14}N^{15}N^{18}O+^{15}N^{14}N^{18}O)$ value.

Summary and Conclusions

We have described techniques to measure six distinct isotope ratios on a single sample of nitrous oxide, including the first measurements of the clumped isotopomers $^{14}N^{15}N^{18}O$ and $^{15}N^{14}N^{18}O$. We have documented the precision and reproducibility of this technique and have introduced the use of activated alumina as a catalyst for equilibration of N_2O to produce standards with elevated and predictable ^{15}N site preference and to calibrate the measurement of $\Delta(^{14}N^{15}N^{18}O+^{15}N^{14}N^{18}O)$ and SP_{18}. Measurements of N_2O produced by a denitrifying bacterium are consistent with a production pathway primarily of irreversible reactions, but with the possibility for some parameters to be set in reversible, equilibrium reactions. These measurements provide the first fingerprint of the composition of clumped isotopologues in a biogenic sample of N_2O. The addition of these isotopic constrains may provide new insights into the environmental sources and sinks of N_2O.

Acknowledgements

This work was supported by a grant from the Gordon and Betty Moore Foundation Marine Microbiology Initiative (Grant #3306) and by NSF-EAR. We thank Dianne Newman for providing the *P. aeruginosa* ΔnosZ mutant and for the use of her laboratory; Sebastian Kopf for aid in microbial culturing; Nami Kitchen for assistance in the laboratory; and Daniel Stolper, Alison Piasecki, and Matthieu Clog for helpful discussions. We thank Karen Casciotti, Shuhei Ono, and Nathaniel Ostrom for providing calibrated reference samples and Sakae Toyoda and

Naohiro Yoshida for measuring the isotopic composition of our reference gas. Finally, we thank Nathaniel Ostrom for helpful comments on an an earlier draft of this manuscript, as well as two anonymous reviewers for their comments.

References

[1] G. Myrhe, D. Shindell, F.-M. Bréon, W. Collins, J. Fuglestvedt, J. Huang, D. Koch, J.-F. Lamarque, D. Lee, B. Mendoza, T. Nakajima, A. Robock, G. Stephens, T. Takemura, H. Zhang. Anthropogenic and Natural Radiative Forcing. In *Climate Change 2013: The Physical Science Basis. Contribution of Working Group I to the Fifth Assessment Report of the Intergovernmental Panel on Climate Change* **2013**, pp. 1–82.

[2] A. R. Ravishankara, J. S. Daniel, R. W. Portmann. Nitrous Oxide (N_2O): The Dominant Ozone-Depleting Substance Emitted in the 21st Century. *Science* **2009**, *326*, 123.

[3] L. Y. Stein, Y. L. Yung. Production, Isotopic Composition, and Atmospheric Fate of Biologically Produced Nitrous Oxide. *Annu. Rev. Earth Planet. Sci.* **2003**, *31*, 329.

[4] W. G. Zumft. Cell Biology and Molecular Basis of Denitrification. *Microbiol. Molec. Biol. Rev.* **1997**, *61*, 533.

[5] T. J. Goreau, W. A. Kaplan, S. C. Wofsy, M. B. McElroy, F. A. Valois, S. W. Watson. Production of NO_2^- and N_2O by Nitrifying Bacteria at Reduced Concentrations of Oxygen. *Appl. Environ. Microbiol.* **1980**, *40*, 526.

[6] A. E. Santoro, C. Buchwald, M. R. McIlvin, K. L. Casciotti. Isotopic Signature of Marine Ammonia-Oxidizing Archaea. *Science* **2011,** *333*, 1282.

[7] C. R. Löscher, A. Kock, M. Könneke, J. LaRoche, H. W. Bange, R. A. Schmitz. Production of oceanic nitrous oxide by ammonia-oxidizing archaea. *Biogeosciences* **2012**, *9*, 2419.

[8] M. Stieglmeier, M. Mooshammer, B. Kitzler, W. Wanek, S. Zechmeister-Boltenstern, A. Richter, C. Schleper. Aerobic nitrous oxide production through N-nitrosating hybrid formation in ammonia-oxidizing archaea. *ISME J.* **2014,** *8*, 1135.

[9] W. Martens-Habbena, W. Qin, R. E. A. Horak, H. Urakawa, A. J. Schauer, J W. Moffett, E. V. Armbrust, A. E. Ingalls, A. H. Devol, D. A. Stahl. The production of nitric oxide by marine ammonia-oxidizing archaea and inhibition of archaeal ammonia oxidation by a nitric oxide scavenger. *Environ. Microbiol.* **2015,** *17*, 2261.

[10] J. A. Kozlowski, M. Stieglmeier, C. Schleper, M. G. Klotz, L. Y. Stein. Pathways and key intermediates required for obligate aerobic ammonia-dependent chemolithotrophy in bacteria and Thaumarchaeota. *ISME J.* **2016,** DOI:10.1038/ismej.2016.2

[11] L. Hink, G. W. Nichol, J. I. Prosser. Archaea produce lower yields of N_2O than bacteria during aerobic ammonia oxidation in soil. *Environ. Microbiol.* **2016,** DOI:10.1111/1462-2920.13282.

[12] N. Wrage, G. L. Veltholf, M. L. van Beusichem, O. Oenema. Role of nitrifier denitrification in the production of nitrous oxide. *Soil Biol. Biochem.* **2001**, *33*, 1723.

[13] J. Heil, B. Wolf, N. Brüggemann, L. Emmenegger, B. Tuzson, H. Vereecken, J. Mohn. Site-specific ^{15}N isotopic signatures of abiotically produced N_2O. *Geochim. Cosmochim. Acta* **2014,** *139*, 72.

[14] W. F. Harper Jr., Y. Takeuchi, S. Riya., M. Hosomi, A. Terada. Novel abiotic reactions increase nitrous oxide production during partial nitrification: Modeling and experiments. *Chem. Engineer. J.* **2015,** *281,* 1017.
[15] X. Zhu-Barker, A. R. Cavazos, N. E. Ostrom, W. R. Horwath, J. B. Glass. The importance of abiotic reactions for nitrous oxide production. *Biogeochem.* **2015,** *126*, 251.
[16] C. Buchwald, K. Grabb, C. M. Hansel, S. D. Wankel. Constraining the role of iron in environmental nitrogen transformations: Dual stable isotope systematics of abiotic NO_2^- reduction by Fe(II) and its production of N_2O. *Geochim. Cosmochim. Acta* **2016,** *186*, 1.
[17] D. Fowler, K. Pilegaard, M. A. Sutton, P. Ambus, M. Raivonen, J. Duyzer, D. Simpson, H. Fagerli, S. Fuzzi, J. K. Schjoerring, C. Granier, A. Neftel, I. S. A. Isaksen, P. Laj, M. Maione, P. S. Monks, J. Burkhardt, U. Daemmgen, J. Neirynck, E. Personne, R. Wichink-Kruit, K. Butterbach-Bahl, C. Flechard, J. P. Tuovinen, M. Coyle, G. Gerosa, B. Loubet, N. Altimir, L. Gruenhage, C. Ammann, S. Cieslik., E. Paoletti, T. N. Mikkelsen, H. Ro-Poulsen, P. Cellier, J. N. Cape, L. Horváth, F. Loreto, Ü Niinemets, P. I. Palmer, J. Rinne, P. Misztal, E. Nemitz, D. Nilsson, S. Pryor, M. W. Gallagher, T. Vesala, U. Skiba, N. Brüggemann, S. Zechmeister-Boltenstern, J. Williams., C. O. Dowd, M. C. Facchini, G. de Leeuw, A. Flossman, N. Chaumerliac, J. W. Erisman. Atmospheric composition change: Ecosystems–Atmosphere interactions. *Atmos. Environ.* **2009**, *43*, 5193.
[18] N. Yoshida. ^{15}N-depleted N_2O as a product of nitrification. *Nature* **1988**, *335*, 528.
[19] K. Kim, H. Craig. Nitrogen-15 and Oxygen-18 Characteristics of Nitrous Oxide: A Global Perspective. *Science* **1993**, *262*, 1855.
[20] D. M. Snider, J. J. Venkiteswaran, S. L. Schiff, J. Spoelstra. Deciphering the oxygen isotopic composition of nitrous oxide produced by nitrification. *Global Change Biol.* **2012,** *18*, 356.
[21] D. M. Snider, J. J. Venkiteswaran, S. L. Schiff, J. Spoelstra. A new mechanistic model of δ^{18}O-N_2O formation by denitrification. *Geochim. Cosmochim. Acta* **2013**, *112*, 102.
[22] L. Rohe, T.-H. Anderson, G. Braker, H. Flessa, A. Giesemann, N. Wrage-Mönnig, R. Well. Fungal oxygen exchange between denitrification intermediates and water. *Rapid Commun. Mass Spectrom.* **2013**, *28*, 377.
[23] S. S. Cliff, M. Thiemens. The ^{18}O/^{16}O and ^{17}O/^{16}O Ratios in Atmospheric Nitrous Oxide: A Mass-Independent Anomaly. *Science* **1997**, *278*, 1774.
[24] D. M. Snider, J. J. Venkiteswaran, S. L. Schiff, J. Spoelstra. From the Ground Up: Global Nitrous Oxide Sources are Constrained by Stable Isotope Values. *PLoS ONE* **2015,** DOI:10.1371/journal.pone.0118954.
[25] C. Brenninkmeijer, T. Röckmann. Mass spectrometry of the intramolecular nitrogen isotope distribution of environmental nitrous oxide using fragment-ion analysis. *Rapid Commun. Mass Spectrom.* **1999**, *13*, 2028.
[26] S. Toyoda, N. Yoshida. Determination of Nitrogen Isotopomers of Nitrous Oxide on a Modified Isotope Ratio Mass Spectrometer. *Anal. Chem.* **1999**, *71*, 4711.
[27] R. Sutka, N. Ostrom, P. Ostrom, H. Gandhi, J. Breznak. Nitrogen isotopomer site preference of N_2O produced by Nitrosomonas europaea and Methylococcus capsulatus Bath. *Rapid Commun. Mass Spectrom.* **2003**, *17*, 738.
[28] R. Sutka, N. Ostrom, P. Ostrom, J. Breznak, H. Gandhi, A. Pitt, F. Li. Distinguishing nitrous oxide production from nitrification and denitrification on the basis of isotopomer abundances. *Appl. Environ. Microbiol.* **2006**, *72*, 638.
[29] C. Frame, K. L. Casciotti Biogeochemical controls and isotopic signatures of nitrous oxide

production by a marine ammonia-oxidizing bacterium. *Biogeosciences* **2010**, *7*, 2695.
[30] N. E. Ostrom, R. L. Sutka, P. H. Ostrom, A. S. Grandy, K. M. Huizinga, H. Gandhi, J. C. von Fischer, G. P. Robertson. Isotopologue data reveal bacterial denitrification as the primary source of N_2O during a high flux event following cultivation of a native temperate grassland. *Soil Biol. Biochem.* **2010**, *42*, 499.
[31] R. L. Sutka, G. C. Adams, N. E. Ostrom, P. H. Ostrom. Isotopologue fractionation during N_2O production by fungal denitrification. *Rapid Commun. Mass Spectrom.* **2008**, *22*, 3989.
[32] T. Kato, S. Toyoda, N. Yoshida, Y. Tang, E. Wada. Isotopomer and isotopologue signatures of N_2O produced in alpine ecosystems on the Qinghai-Tibetan Plateau. *Rapid Commun. Mass Spectrom.* **2013**, *27*, 1517.
[33] S. Toyoda, N. Yoshida, K. Koba. Isotopocule Analysis of Biologically Produced Nitrous Oxide in Various Environments. *Mass Spectrom. Rev.* **2015,** DOI:10.1002/mas.21459.
[34] C. H. Frame, E. Deal, C. D. Nevison, K. L. Casciotti. N_2O production in the eastern South Atlantic: Analysis of N_2O stable isotopic and concentration data. *Global Biogeochem. Cycles* **2014,** *28*, 1262.
[35] N. Yoshida, S. Toyoda. Constraining the atmospheric N_2O budget from intramolecular site preference in N_2O isotopomers. *Nature* **2000**, *405*, 330.
[36] S. Park, R. Croteau, K. A. Boering, D. M. Etheridge, D. Ferretti, P. J. Fraser, K.-R. Kim, P. B. Krummel, R. L. Langenfelds, T. D. van Ommen, L. P. Steele, C. M. Trudinger. Trends and seasonal cycles in the isotopic composition of nitrous oxide since 1940. *Nat. Geosci.* **2012**, *5*, 261.
[37] J. M. Eiler. "Clumped-isotope" geochemistry—The study of naturally-occurring, multiply-substituted isotopologues. *Earth Planet. Sci. Lett.* **2007**, *62*, 309.
[38] J. M. Eiler. The Isotopic Anatomies of Molecules and Minerals. *Annu. Rev. Earth Planet. Sci.* **2013**, *41*, 411.
[39] J. M. Eiler, E. A. Schauble. $^{18}O^{13}C^{16}O$ in Earth's atmosphere. *Geochim. Cosmochim. Acta* **2004**, *68*, 4767.
[40] D. A. Stolper, A. L. Sessions, A. A. Ferreira, E. V. Santos Neto, A. Schimmelmann, S. S. Shusta, D. L. Valentine, J. M. Eiler. Combined ^{13}C–D and D–D clumping in methane: Methods and preliminary results. *Geochim. Cosmochim. Acta* **2014**, *126*, 169.
[41] L. Y. Yeung, E. D. Young, E. A. Schauble. Measurements of $^{18}O^{18}O$ and $^{17}O^{18}O$ in the atmosphere and the role of isotope-exchange reactions. *J. Geophys. Res.* **2012**, *117*, D18306.
[42] P. Ghosh, J. F. Adkins, H. P. Affek, B. Balta, W. Guo, E. A. Schauble, D. P. Schrag, J. M. Eiler. ^{13}C-^{18}O bonds in carbonate minerals: A new kind of paleothermometer. *Geochim. Cosmochim. Acta* **2006**, *70*, 1439.
[43] D. A. Stolper, M. Lawson, C. L. Davis, A. A. Ferreira, E. V. Santos Neto, G. S. Ellis, M. D. Lewan, A. M. Martini, Y. Tang, M. Schoell, A. L. Sessions, J. M. Eiler. Formation temperatures of thermogenic and biogenic methane. *Science* **2014**, *344*, 1500.
[44] M. Daeron, W. Guo, J. Eiler, D. Genty, D. Blamart, R. Boch, R. Drysdale, R. Maire, K. Wainer, G. Zanchetta. $^{13}C^{18}O$ clumping in speleothems: Observations from natural caves and precipitation experiments. *Geochim. Cosmochim. Acta* **2011**, *75*, 3303.
[45] M. Clog M., A. Martini, M. Lawson, J. Eiler. Doubly ^{13}C-substituted ethane in shale gases, Goldschmidt Conference. *Mineralogical Magazine,* **2014**, Sacramento, CA, p. 435.
[46] L. Y. Yeung, J. L. Ash, E. D. Young. Biological signatures in clumped isotopes of O_2. *Science* **2015**, *348*, 431.
[47] D. T. Wang, D. S. Gruen, B. S. Lollar, K.-U. Hinrichs, L. C. Stewart, J. F. Holden, A. N.

Hristov J. W. Pohlman, P.L. Morrill, M. Könneke, K. B. Delwiche, E. P. Reeves, C. N. Sutcliffe, D. J. Ritter, J. S. Seewald, J. C. McIntosh, H. F. Hemond, M. D. Kubo, D. Cardace, T. M. Hoeher, S. Ono. Nonequilibrium clumped isotope signals in microbial methane. *Science* **2015**, *348*, 428.

[48] J. Kaiser, T. Röckmann, C. A. M. Brenninkmeijer. Assessment of $^{15}N^{15}N^{16}O$ as a tracer of stratospheric processes. *Geophys. Res. Lett.* **2003**, *30*, 1046.

[49] J. M. Eiler, M. Clog, P. Magyar, A. Piasecki, A. Sessions, D. Stolper, M. Deerberg, H.-J. Schlueter, J. Schwieters. A high-resolution gas-source isotope ratio mass spectrometer. *Int. J. Mass Spectrom.* **2013**, *35*, 45.

[50] Z. Wang, E. A. Schauble, J. M. Eiler. Equilibrium thermodynamics of multiply substituted isotopologues of molecular gases. *Geochim. Cosmochim. Acta* **2004**, *68*, 4779.

[51] M. A.Webb, T. F. Miller. Position-specific and clumped stable isotope studies: comparison of the urey and path-integral approaches for carbon dioxide, nitrous oxide, methane, and propane. *J. Phys. Chem. A* **2014**, *118*, 467.

[52] J. Bigeleisen, L. Friedman. The Infra-Red Spectra of $N^{15}N^{14}O^{16}$ and $N^{14}N^{15}O^{16}$. Some Thermodynamic Properties of the Isotopic N_2O Molecules. *J. Chem. Phys.* **1950**, *18*, 1656.

[53] J. Bigeleisen, M. Mayer. Calculation of equilibrium constants for isotopic exchange reactions. *J. Chem. Phys.* **1947**, *15*, 261.

[54] H. C. Urey. The thermodynamic properties of isotopic substances. *J. Chem. Soc.* **1947**, 562.

[55] L. Y. Yeung, J. L. Ash, E. D. Young. Rapid photochemical equilibration of isotope bond ordering in O_2. *J. Geophys Res. Atmos.* **2014**, *119,* 10522.

[56] K. J. Dennis, H. P. Affek, B. H. Passey, D. P. Schrag, J. M. Eiler. Defining an absolute reference frame for 'clumped' isotope studies of CO_2. *Geochim. Cosmochim. Acta* **2011**, *75*, 7117.

[57] D. A. Stolper, A. M. Martini, M. Clog, P. M. Douglas, S. S. Shusta, D. L. Valentine, A. L. Sessions, J. M. Eiler. Distinguishing and understanding thermogenic and biogenic sources of methane using multiply substituted isotopologues. *Geochim. Cosmochim. Acta* **2015**, *161*, 219.

[58] E. R. S. Winter. The Decomposition of N_2O on Oxide Catalysts III. The Effect of O_2. *J. Catal.* **1974**, *34*, 431.

[59] E. R. S. Winter. The Decomposition of Nitrous Oxide on Metallic Oxides. *J. Catal.* **1970**, *19*, 32.

[60] H. Craig. The geochemistry of the stable carbon isotopes. *Geochim. Cosmochim. Acta* **1953**, *3*, 53.

[61] T. E. Cerling, D. K. Solomon, J. Quade, J. R. Bowman. On the isotopic composition of carbon in soil carbon dioxide. *Geochim. Cosmochim. Acta* **1991**, *55*, 3403.

[62] L. Friedman, J. Bigeleisen. Oxygen and Nitrogen Isotope Effects in the Decomposition of Ammonium Nitrate. *J. Chem. Phys.* **1950**, *18*, 1325.

[63] M. Westley, B. Popp, T. Rust. The calibration of the intramolecular nitrogen isotope distribution in nitrous oxide measured by isotope ratio mass spectrometry. *Rapid Commun. Mass Spectrom.* **2007**, *21*, 391.

[64] S. Park, E. L. Atlas, K. A. Boering. Measurement of N_2O isotopologues in the stratosphere: Influence of transport on the apparent enrichment factors and the isotopologue fluxes to the troposphere. *J. Geophys. Res.* **2004**, *109*, D01305, DOI:10.1029/2003JD003731.

[65] E. Harris, D. D. Nelson, W. Olszewski, M. Zahniser, K. E. Potter, B. J. McManus, A. Whitehill, R. G. Prinn, S. Ono. Development of a Spectroscopic Technique for Continuous

Online Monitoring of Oxygen and Site-Specific Nitrogen Isotopic Composition of Atmospheric Nitrous Oxide. *Anal. Chem.* **2014,** *86*, 1726.

[66] J. Mohn, B. Wolf, S. Toyoda S., C.-T. Lin, M. C. Liang, N. Brüggemann, H. Wissel, A. E. Steiker, J. Dyckmans, L. Szwec, N. E. Ostrom, K. L. Casciotti, M. Forbes, A. Giesemann, R. Well, R. R. Doucett, C. T. Yarnes, A. R. Ridley, J. Kaiser, N. Yoshida. Interlaboratory assessment of nitrous oxide isotopomer analysis by isotope ratio mass spectrometry and laser spectroscopy: current status and perspectives. *Rapid Commun. Mass Spectrom.* **2014**, *28*, 1995.

[67] N. E. Ostrom, A. Pitt, R. Sutka, P. H. Ostrom, A. S. Grandy, K. M. Huizinga, G. P. Robertson. Isotopologue effects during N_2O reduction in soils and in pure cultures of denitrifiers. *J.Geophys. Res.* **2007**, *112*, G02005, DOI:10.1029/2006JG000287.

[68] D. M. Kool, N. Wrage, O. Oenema, D. Harris, J. W. Van Groenigen. The ^{18}O signature of biogenic nitrous oxide is determined by O exchange with water. *Rapid Commun. Mass Spectrom.* **2009**, *23*, 104.

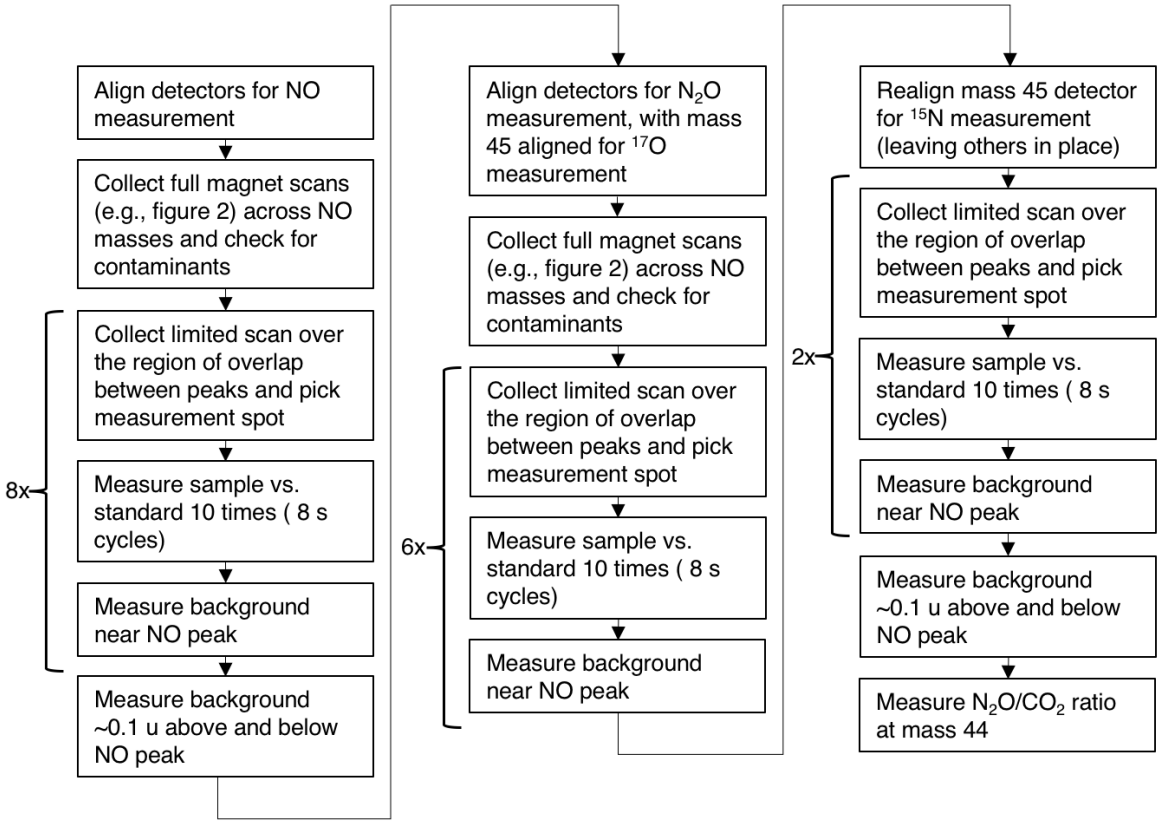

Figure 1. A flow chart of the steps required for the measurement of a sample.

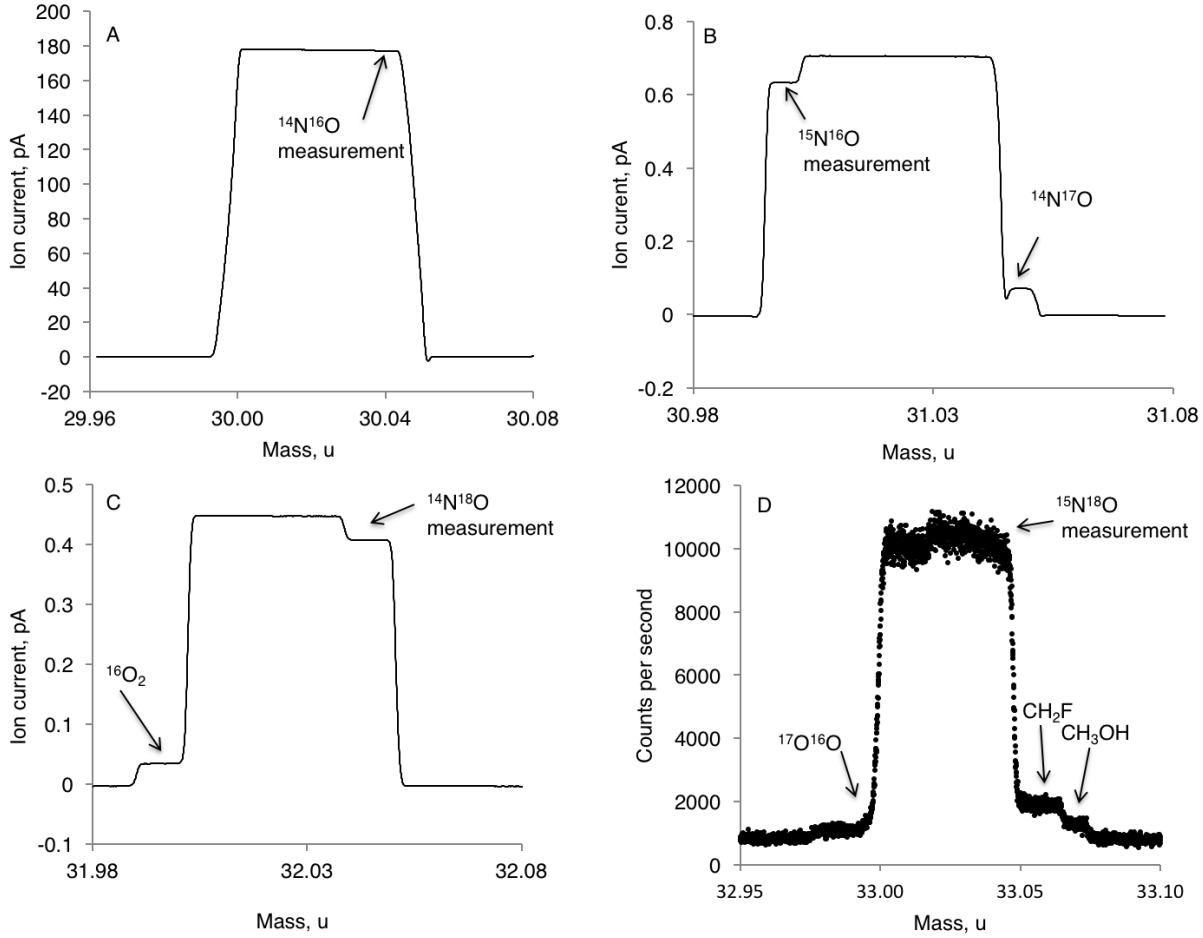

Figure 2. Mass spectra of the NO fragment of N_2O, collected by varying the magnet setting of the mass spectrometer. On each spectrum the position of measurement is indicated, as are other isotopologues of NO and contaminating species. (A) Mass 30. (B) Mass 31. (C) Mass 32. (D) Mass 33.

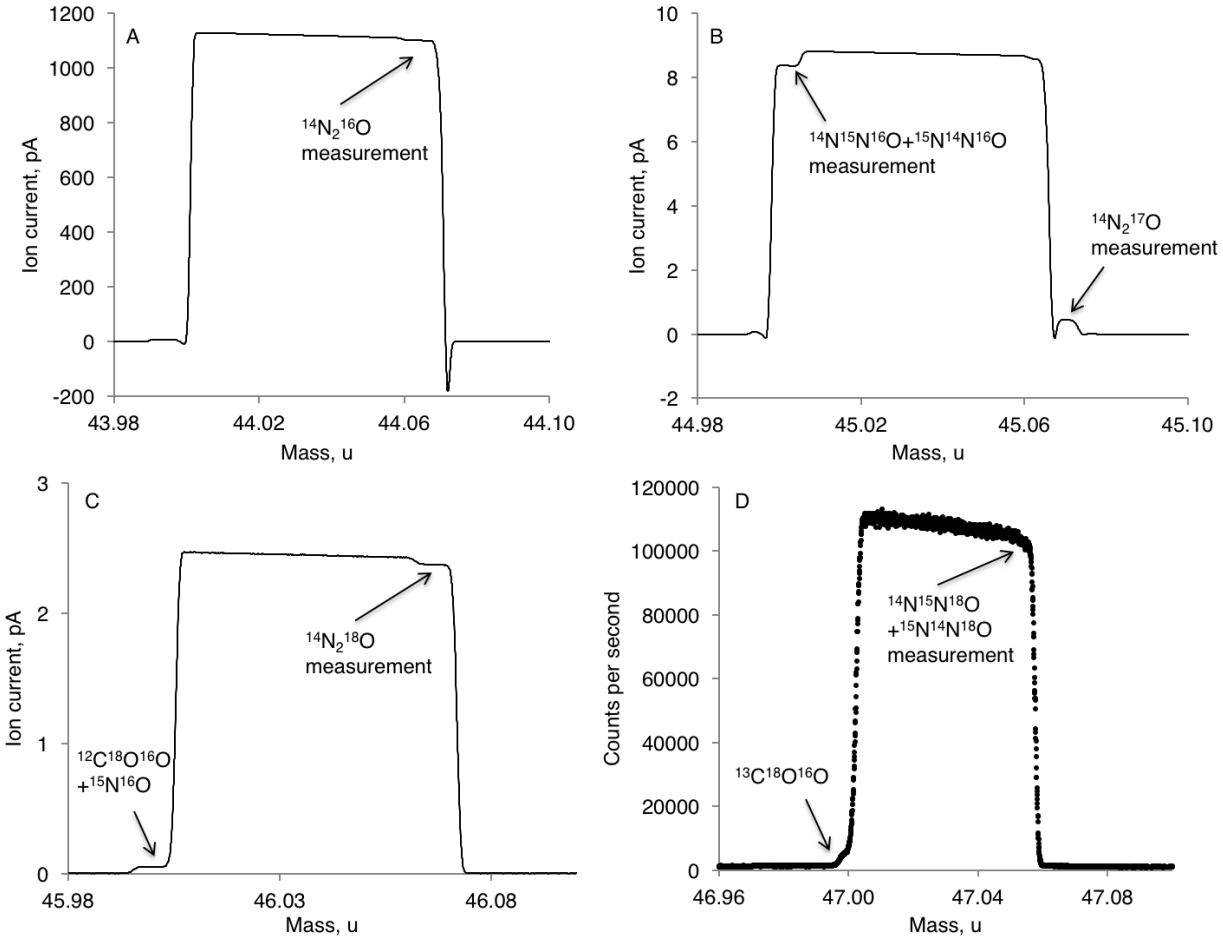

Figure 3. Mass spectra of of N_2O. On each spectrum the position of measurement is indicated, as are other isotopologues of N_2O and contaminating species. (A) Mass 44. (B) Mass 45. (C) Mass 46. (D) Mass 47.

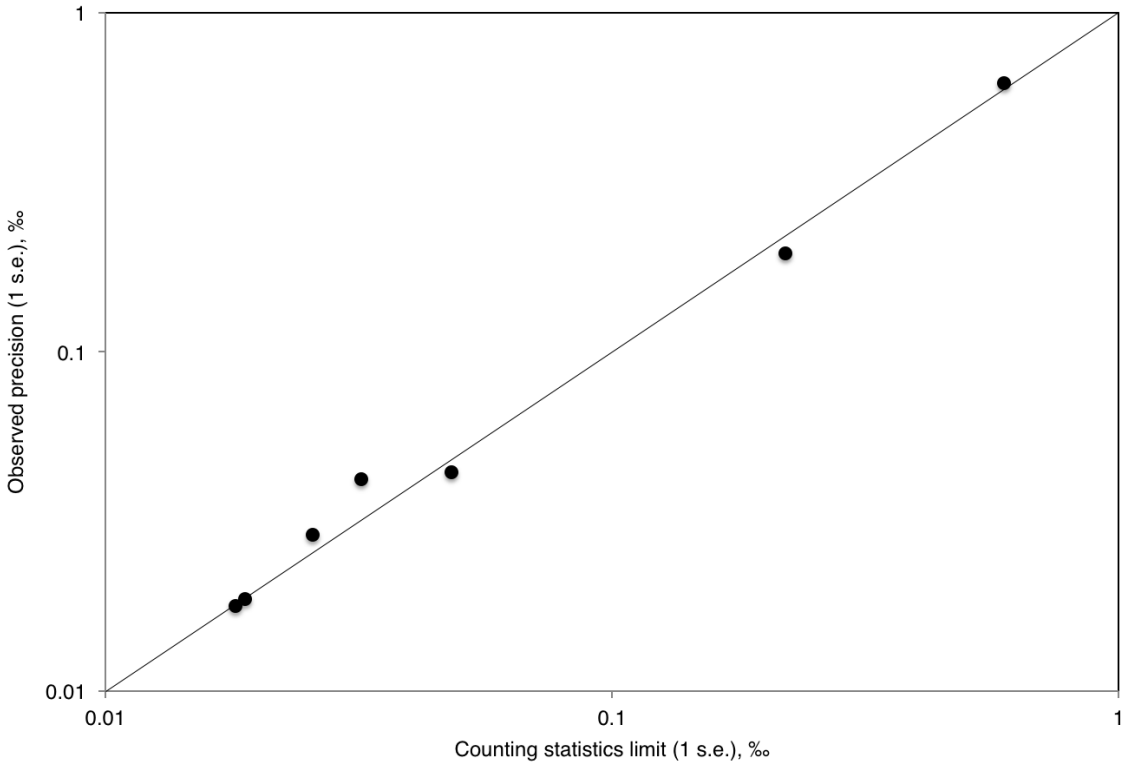

879
880 Figure 4. Comparison of observed internal precision and the counting statistics limit. Each point
881 represents the standard error for one complete measurement of a single isotopic ratio in a typical
882 sample. As is expected from counting statistics, more abundant isotopologues are observed with
883 greater precision.
884

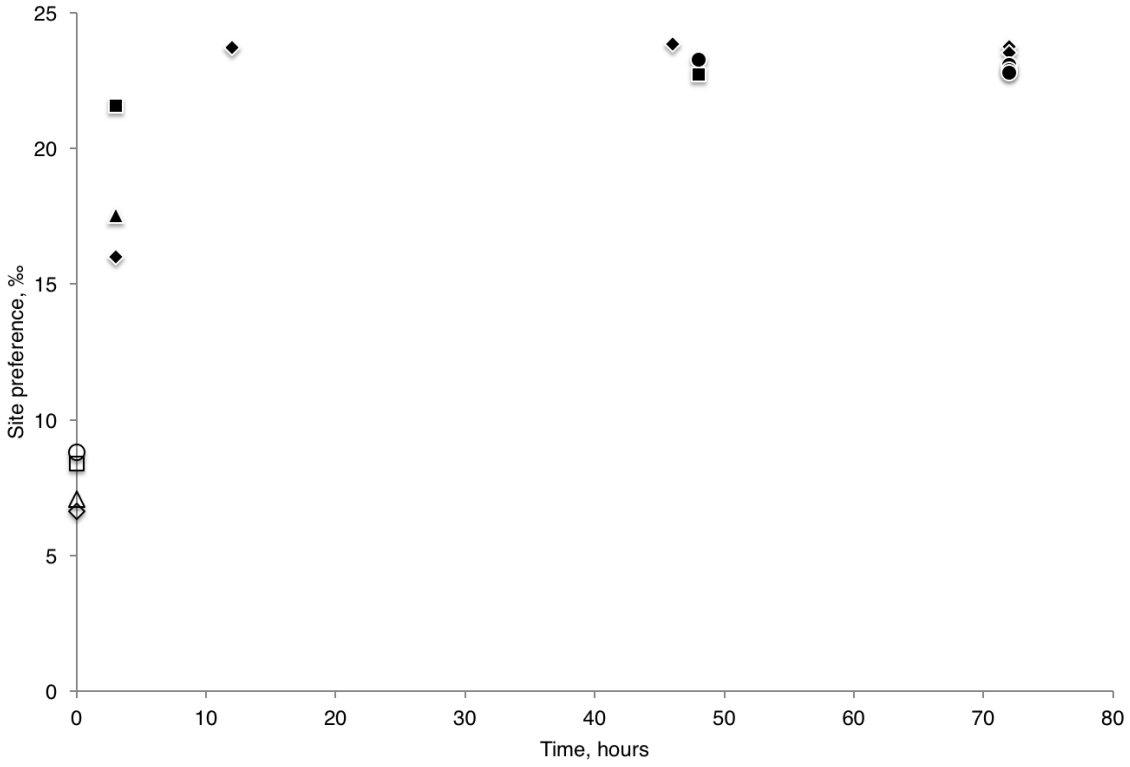

Figure 5. Behavior of SP upon heating at 200°C in the presence of a catalyst. Hollow symbols represent starting compositions; filled symbols represent the composition of equivalent samples after heating at 200°C in the presence of a catalyst for 3-72 h, as marked. All samples use the reference gas calibration and correction for scrambling that is described in the main text. All samples heated for >12 hours have reached a common, time-invariant composition. 1 s.e. mass spectrometric error bars are smaller than each point.

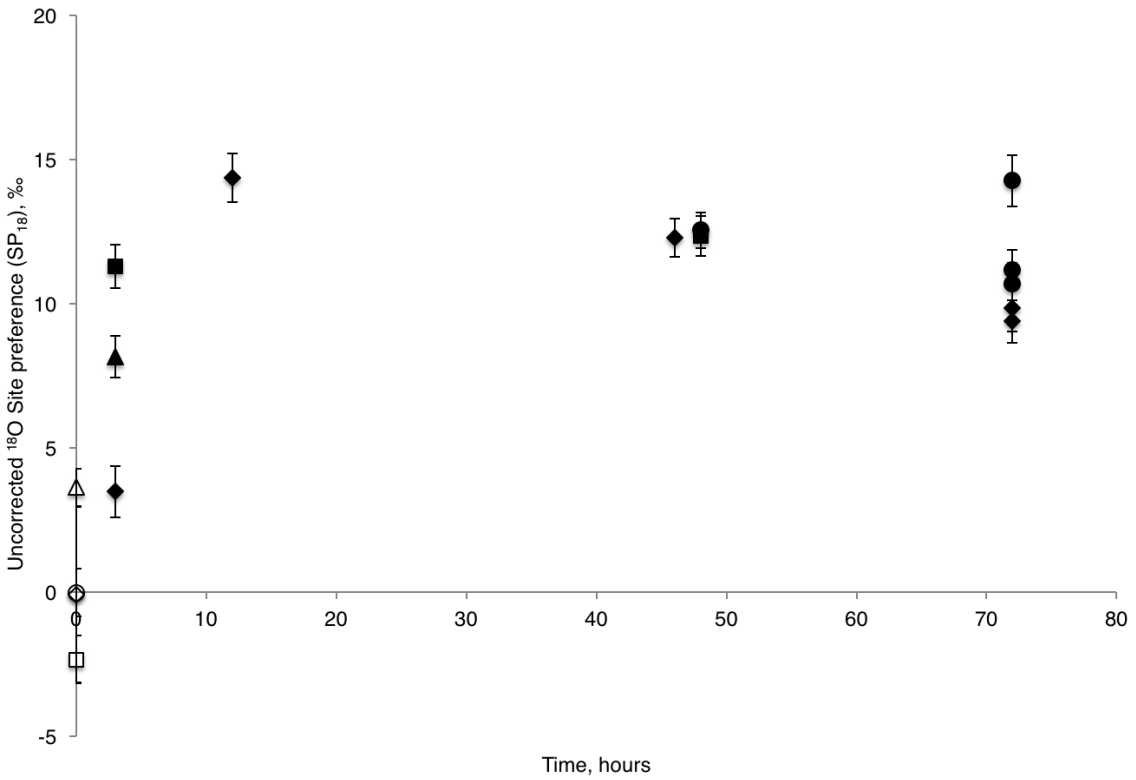

Figure 6. Behavior of SP_{18} upon heating at 200°C in the presence of a catalyst. Symbols are the same as in Fig. 4. Samples are reported relative to the internal working N_2O standard. Again, all samples that have been heated in the presence of a catalyst have reached a common, time-invariant composition. These results are used to determine the rearrangement correction and reference gas composition for $^{14}N^{15}N^{18}O$ and $^{15}N^{14}N^{18}O$, as described in the main text. Error bars represent 1 s.e. mass spectrometric error.

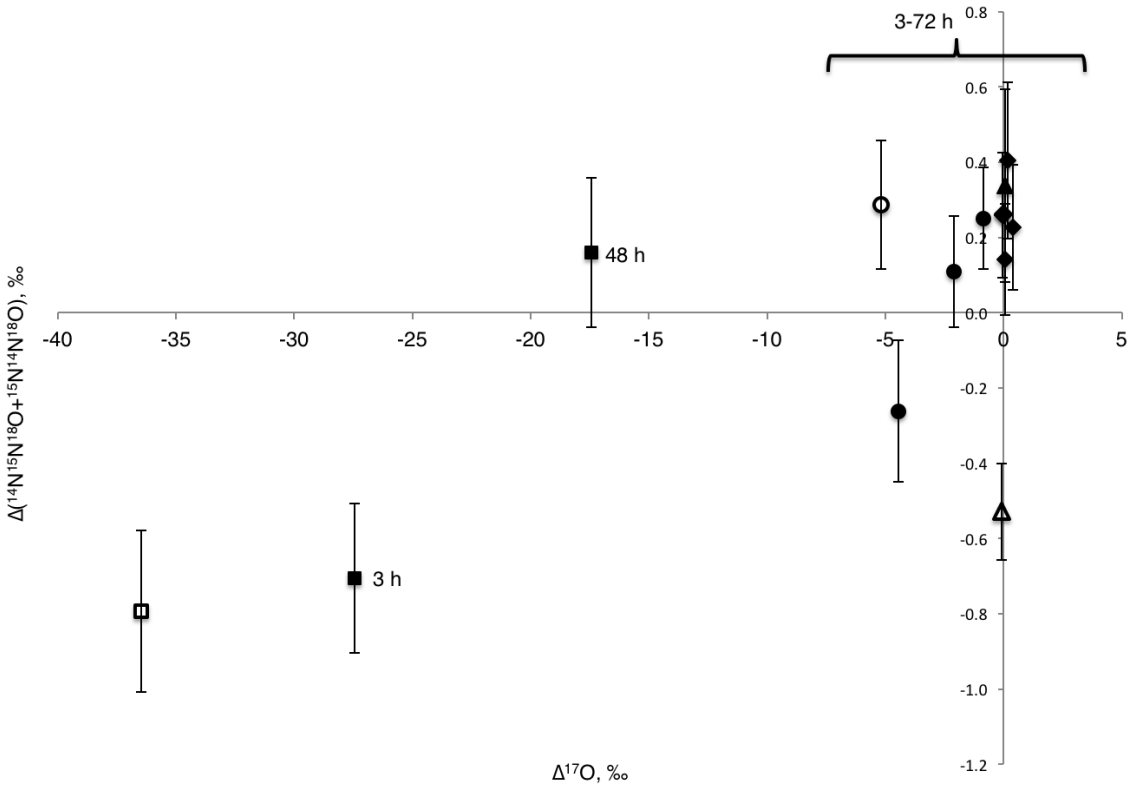

Figure 7. Behavior of $\Delta^{17}O$ and $\Delta(^{14}N^{15}N^{18}O+^{15}N^{14}N^{18}O)$ upon heating at 200°C. Symbols are the same as in Fig. 4. Gases of all starting compositions converge at a common value of $\Delta(^{14}N^{15}N^{18}O+^{15}N^{14}N^{18}O)$. Samples that begin at $\Delta^{17}O > 0$ approach but do not reach $\Delta^{17}O = 0$, suggesting that position-specific and clumped isotopologues can be fully equilibrated even without all O atoms experiencing exchange. Error bars represent 1 s.e. mass spectrometric error.

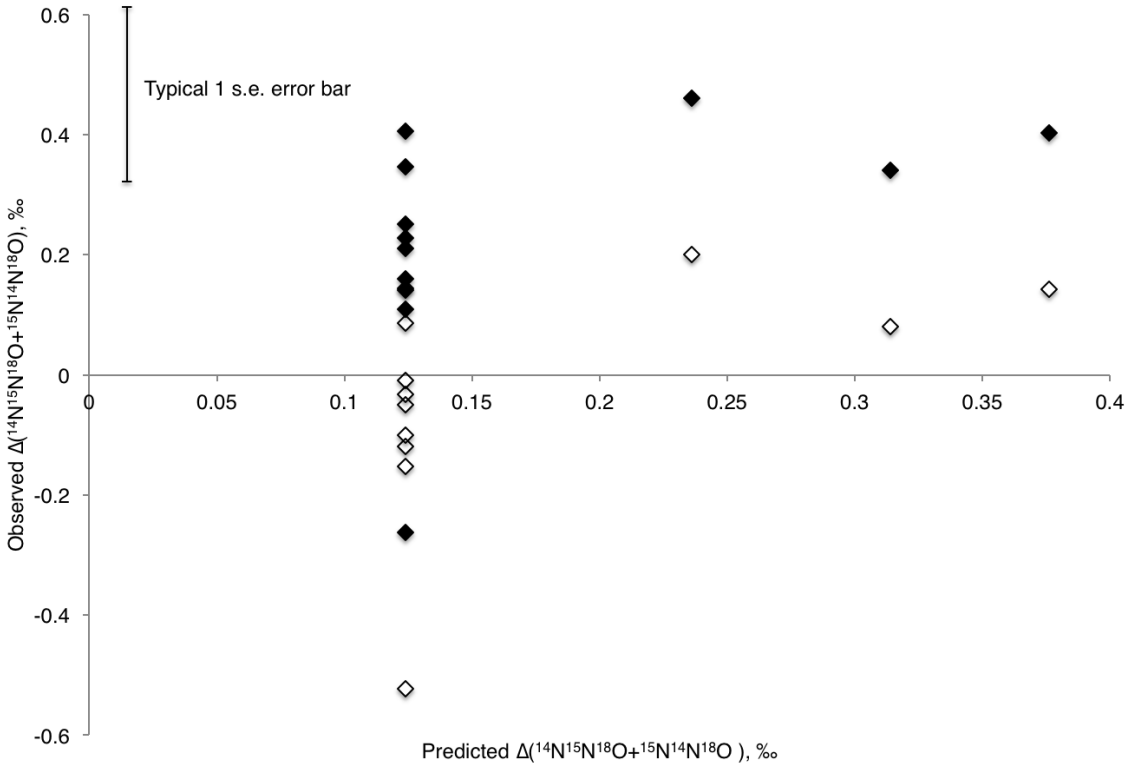

Figure 8. Measured $\Delta(^{14}N^{15}N^{18}O+^{15}N^{14}N^{18}O)$ compared to statistical mechanical predictions. Samples were heated at 200°C, 93°C, 50°C, and 25°C, which each decrease in temperature leading to an increase in the predicted $\Delta(^{14}N^{15}N^{18}O+^{15}N^{14}N^{18}O)$, but with no significant change in the observed property. Hollow symbols are reported against the internal reference gas; filled symbols have been corrected for the composition of the reference N_2O, as described in the main text. For clarity, the typical 1 s.e. error envelope of ±0.15‰ is shown.

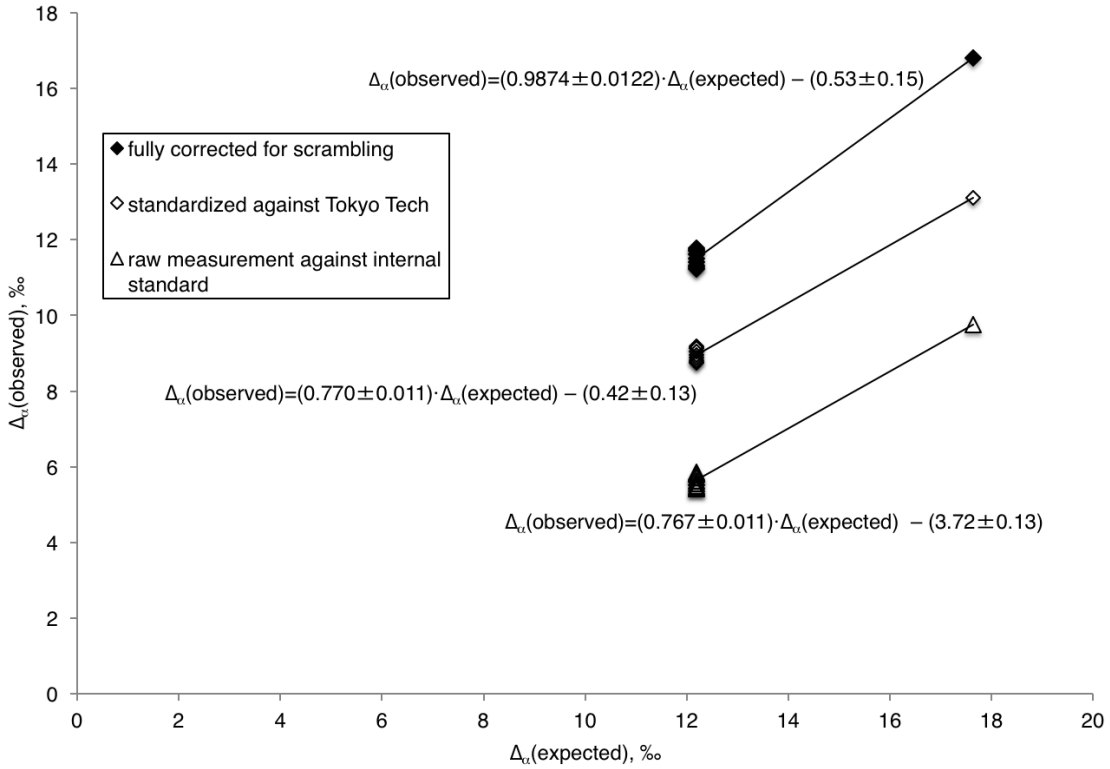

Figure 9. Measured Δ_α compared to statistical mechanical predictions. Samples are the same as those in Fig. 7 (heated to 200°C and 93°C), as described in the text; with decreasing temperature both observed and predicted values of Δ_α increase. Hollow triangles represent uncorrected measurements reported against internal standard. Hollow diamonds have been adjusted to the scale of $\delta^{15}N$ vs. N_2 in air through calibration of the internal standard by S. Toyoda and N. Yoshida, Tokyo Tech. Filled diamonds have been corrected for scrambling by the additional measurement of a secondary standard provided by S. Ono, MIT, as described in the main text. All corrections are independent of the results of the equilibration experiments reported here.

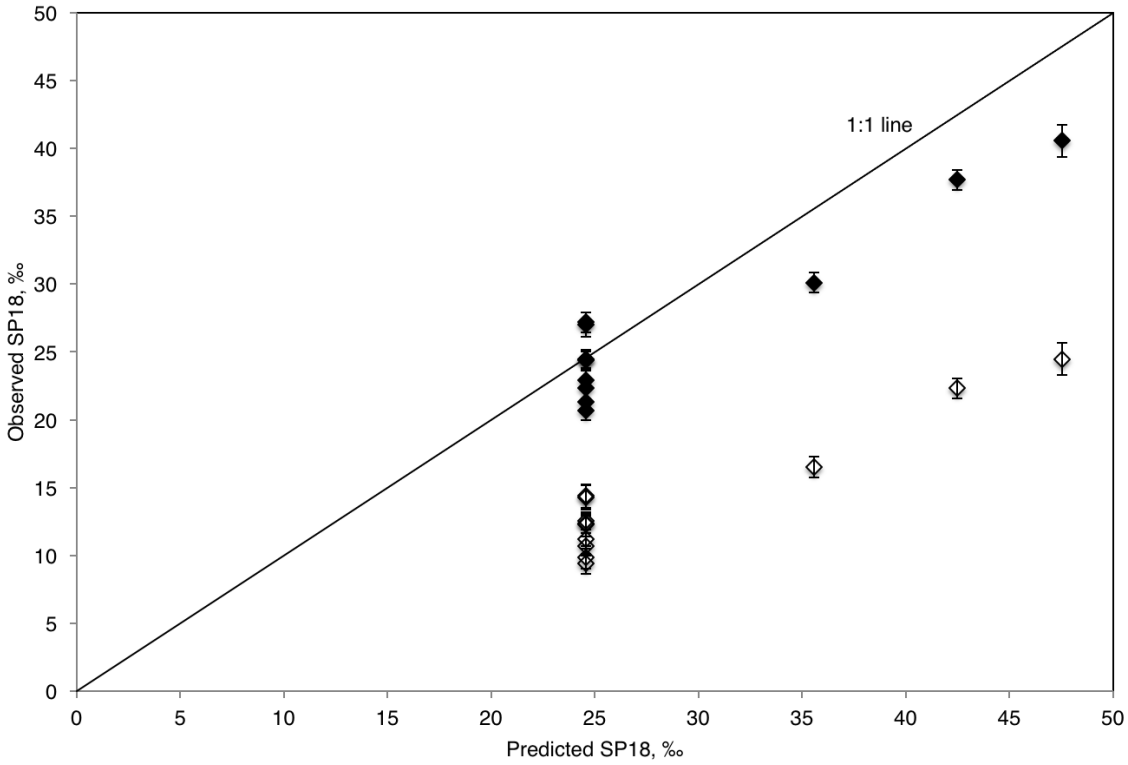

Figure 10. Measured SP_{18} compared to statistical mechanical predictions. Samples were heated at 200°C, 93°C, 50°C, and 25°C, as described in the text; with decreasing temperature both observed and predicted values of $\Delta(^{14}N^{15}N^{18}O)$ increase. Hollow symbols represent uncorrected measurements, reported against the internal reference gas. The corrected results (filled symbols) are adjusted using a value *f* of 0.77 and an SP_{18} of the reference gas chosen to make the average value measured at 200°C match the statistical mechanical prediction (see Table 5). These results suggest that the quantity SP_{18} has approached but not reached equilibrium for experiments at 25°C-93°C. 1 s.e. error bars are shown for each point.

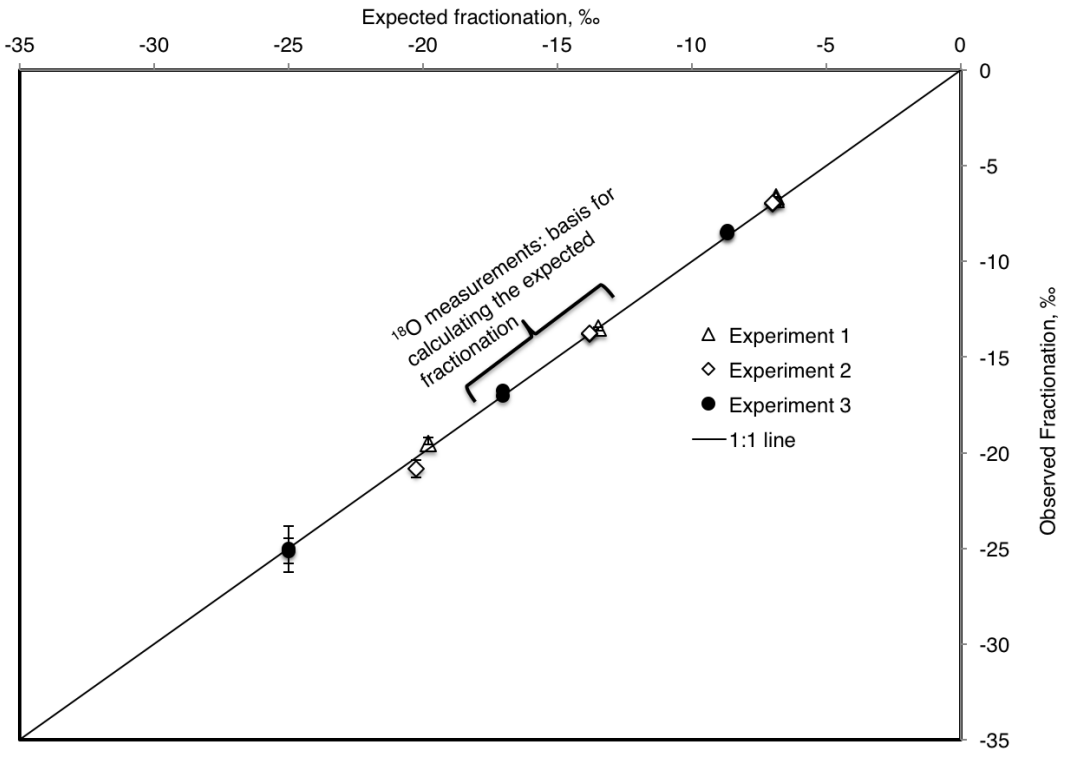

Figure 11. Comparison of the observed and expected fractionation for diffused N_2O. Experiments 1 and 2 were conducted before establishment of complete background and cleaning procedures for eliminating or correcting for isobaric interferences to $^{14}N_2{}^{17}O$ and $^{14}N^{15}N^{18}O$. Observed fractionations are interpreted to differ from experiment to experiment because of varying contributions from gas-phase interdiffusion and Knudsen diffusion

Cardinal Mass	Isotopic Variant	Mass (u)	Proportional abundance[a]
44	$^{14}N_2{}^{16}O$	44.0011	$9.90x10^{-1}$
45	$^{14}N^{15}N^{16}O$	44.9981	$3.64x10^{-3}$
	$^{15}N^{14}N^{16}O$	44.9981	$3.64x10^{-3}$
	$^{14}N_2{}^{17}O$	45.0053	$3.83x10^{-4}$
46	$^{15}N^{15}N^{16}O$	45.9951	$1.34x10^{-5}$
	$^{14}N^{15}N^{17}O$	46.0023	$1.41x10^{-6}$
	$^{15}N^{14}N^{17}O$	46.0023	$1.41x10^{-6}$
	$^{14}N_2{}^{18}O$	46.0053	$1.99x10^{-3}$
47	$^{15}N^{15}N^{17}O$	46.9993	$5.17x10^{-8}$
	$^{14}N^{15}N^{18}O$	47.0023	$7.30x10^{-6}$
	$^{15}N^{14}N^{18}O$	47.0023	$7.30x10^{-6}$
48	$^{15}N^{15}N^{18}O$	47.9994	$2.68x10^{-8}$

Table 1

Masses and abundances of the isotopic variants of N_2O.

[a]Calculated for a sample of N_2O with a random distribution of rare isotopes and with $\delta^{15}N$=0‰ relative to Air-N_2 and $\delta^{17}O$ and $\delta^{18}O$=0‰ relative to VSMOW.

	$\delta^{15}N$, ‰			$\delta^{18}O$, ‰			$\delta^{15}N^{\alpha}$, ‰		
Sample	Meas.	+/-	Reported	Meas.	+/-	Reported	Meas.	+/-	Reported
MSU (n=4)	-0.86	0.15	-0.9	38.67	0.22	38.5	0.23	0.20	0.7
MIT (n=4)	0.00	0.25	-0.24	40.76	0.40	40.43	-0.07	0.17	-0.78
Stanford (n=1)	0.27		0.31	40.59		40.85	0.76		-0.31

Table 2

Isotopic composition of standard gases, as measured versus Caltech internal reference gas and referenced to international standards (N_2 in air for $\delta^{15}N$ and VSMOW for $\delta^{18}O$ as described in the main text. Uncertainties are calculated as 1 standard deviation for the analysis of replicate samples. Reported values are the composition of each standard gas as determined by Tokyo Tech.

	Average (n=4)	+/- (1 s.d.)
$\Delta(^{14}N^{15}N^{18}O+^{15}N^{14}N^{18}O)$	0.44	0.26
$\Delta(^{14}N^{15}N^{18}O)$	2.50	0.30
SP_{18}	3.61	0.86

960
961
962 Table 3
963 Average of repeated measurements of MSU reference gas between July 2012 and August 2014,
964 corrected and standardized as described in the Reproducibility and Standardization section of the
965 main text.
966

967

			^{15}N site preference, ‰			Difference between SP at given T and 200°C	
T,°C	Time, h		Measured	+/- (1 s.d.)	Predicted[a]	Measured	Predicted
200	12-72	n = 8	23.28	0.43	24.37	—	—
93	143	n = 1	34.19		35.28	10.66	10.65
50	146	n = 1	37.26		42.09	13.66	17.28
25	1225	n = 1	39.42		47.12	15.77	22.20

968
969
970 Table 4
971 Comparison of SP for heated N_2O samples and theoretical predictions.
972 [a]Based on Wang et al.;[50] anharmonic partition functions are chosen to best match Webb and
973 Miller.[51]
974
975

	Δ_i(reference), ‰	±, ‰
$^{14}N^{15}N^{18}O$	4.67	1.08
$^{15}N^{14}N^{18}O$	-4.15	1.09
$^{14}N^{15}N^{18}O$+$^{15}N^{14}N^{18}O$	0.26	0.19

Table 5
Reference gas compositions for clumped isotopic measurements of N_2O, based on equilibration experiments. Uncertainties are ±1 standard deviation.

Replicate	$\delta^{15}N$, ‰	+/-	$\delta^{17}O$, ‰	+/-	$\delta^{18}O$, ‰	+/-	SP, ‰	+/-	SP_{18}, ‰	+/-	$\Delta(^{14}N^{15}N^{18}O$-$^{15}N^{14}N^{18}O)$, ‰
1	-5.61	0.02	25.16	0.05	47.80	0.04	-3.91	0.04	2.6	0.8	-0.06
2	-5.32	0.02	24.91	0.07	47.86	0.03	-3.70	0.04	2.8	0.8	0.57
3	-5.32	0.02	25.09	0.04	48.05	0.02	-3.41	0.05	-3.8	0.9	0.67
average	**-5.42**	**0.17**	**25.05**	**0.13**	**47.90**	**0.13**	**-3.67**	**0.25**	**-0.5**	**3.8**	**0.39**

Table 6

Isotopic composition of N_2O produced by replicate cultures of *Pseudomonas aeruginosa,* strain PA14, Δ*nosZ* mutant.